Blue Carbon Accounting Model (BlueCAM) Technical Overview

Prepared for the Clean Energy Regulator, 31 August 2021

Image: C. Lovelock

Authors

Catherine E. Lovelock, The University of Queensland
James Sippo, Southern Cross University
Maria Fernanda Adame, Griffith University
Sabine Dittmann, Flinders University
Sharyn Hickey, The University of Western Australia
Lindsay Hutley, Charles Darwin University
Alice Jones, University of Adelaide
Jeff Kelleway, University of Wollongong
Paul Lavery, Edith Cowan University
Peter Macreadie, Deakin University
Damien Maher, Southern Cross University
Luke Mosely, University of Adelaide
Kerrylee Rogers, University of Wollongong

Table of Contents

General Introduction

The Blue Carbon Accounting Model (BlueCAM) has been developed alongside the draft *Carbon Credits (Carbon Farming Initiative – Tidal Restoration of Blue Carbon Ecosystems) Methodology Determination 2022* (the blue carbon method) and will be used to calculate the net carbon abatement from each of the soil and vegetation sequestration and emissions avoidance components of a project.

For the blue carbon method, the project activity will be to introduce tidal flow resulting in the rewetting of previously completely or partially drained coastal wetland ecosystems. This could involve removing or modifying an entire, or part of a sea wall, bund, drain, or other type of tidal flow restriction device such as a tidal gate.

This document describes an approach to estimating carbon abatement of a project activity. The model-only approach is intended to simplify the requirements of the method and reduce costs associated with sampling.

1.1 Overview – carbon pools and greenhouse gases

The introduction of tidal flows to coastal land can increase carbon sequestration through promoting the growth of blue carbon ecosystems such as mangroves, saltmarsh, seagrass, and supratidal forests comprised of *Melaleuca, Casuarina* and other plant genera. Tidal introduction can also decrease greenhouse gas emissions (GHG) from land through inundation and the increase in salinity in soils and water. BlueCAM considers changes in organic carbon stocks and greenhouse gas emissions following a management intervention of the introduction of tidal flows. The net change in GHG emissions is based on change (reduction) of GHG emissions from land use prior to tidal introduction and from the carbon sequestered and stored in living vegetation (live aboveground biomass), the roots of living vegetation (live belowground biomass) and in soil. Table 1 provides an overview of the carbon pools and greenhouse gases and emissions sources that are relevant to calculating the net abatement amount for a blue carbon project. Carbon in dead organic matter and litter are not included in the blue carbon method because litter carbon stocks are small compared to other pools and may be exported, and dead wood is assumed to have been previously accounted for in aboveground growth (Kennedy et al. 2014; Lasco et al. 2006).

In the BlueCAM all carbon pools or emission sources (Table 1) are estimated for baseline and with-project scenarios using quantitative models which are explained in this Supplementary Information document. As outlined in the table, the modelling of the carbon pools and emissions sources is consistent with Intergovernmental Panel on Climate Change (IPCC) guidance (IPCC 2013, 2019). No measurement of carbon pools or greenhouse gases is required by a proponent (although see the Hydrological Assessment and Monitoring requirements).

Total net abatement is calculated as the sum of avoided emissions from prior (baseline) land-use and the carbon sequestered in coastal wetland biomass and soils, minus the emissions from coastal wetlands and any carbon accumulated in the prior land uses and any fuel use associated with the project activities.

Table 1 Carbon pools and greenhouse gases considered in this method

Overview of gases accounted for in abatement calculations				
Item	Relevant carbon pool or emission source		Greenhouse gas	IPCC guidance
1	Carbon pool	Living aboveground biomass	Carbon dioxide (CO_2)	2013 Wetland Supplement
2	Carbon pool	Living belowground biomass	Carbon dioxide (CO_2)	2013 Wetland Supplement
3	Carbon pool	Soil	Carbon dioxide (CO_2)	2013 Wetland Supplement 2019 Refinement of 2006 Guidance
4	Emission source	Fuel use	Methane (CH_4) Nitrous oxide (N_2O) Carbon dioxide (CO_2)	2019 Refinement of 2006 Guidance
5	Emission source	Flooded land	Methane (CH_4) Nitrous oxide (N_2O)	2019 Refinement of 2006 Guidance
6	Emission source	Aquaculture	Nitrous oxide (N_2O)	2019 Refinement of 2006 Guidance 2013 Wetland Supplement
7	Emission source	Agricultural lands	Nitrous oxide (N_2O) Carbon dioxide (CO_2)	2019 Refinement of 2006 Guidance
8	Emission source	Ecosystem transitions (E_{TR})	Carbon dioxide (CO_2)	2013 Wetland Supplement

1.2 Regional approach – climatic zones

1.2.1 Influence of climate on coastal wetland types

Variation in climate, including variation in humidity, precipitation, groundwater and river flows influences the type (species composition) and biomass of coastal wetland communities which influence organic carbon stocks and fluxes and greenhouse gas fluxes. Climatic regions used in this method broadly follow previous climatic classifications of Australia (Figure 1) and the prior aggregation of Natural Resource Management (NRM) regions by the Australian Government for projecting the influence of climate change on ecosystems and human societies (see Climate Change in Australia's website). The regionalisation scheme was developed by CSIRO in consultation with the Department of the Environment that defined eight NRM clusters. The cluster boundaries were aligned with existing boundaries of 56 NRM regions (Department of Agriculture, 2013, Department of the Environment, 2013). These regions facilitate the development and implementation of strategic NRM plans. NRM groups play key roles in the delivery of government NRM programmes, including programs like the National Landcare Programme. Because of the strong regional variation in climate and its effects on coastal wetlands BlueCAM uses these climatic regions to estimate regionally specific abatement.

Freshwater availability influences soil water content and soil salinity which are strong determinants of plant community composition and productivity. For example, groundwater availability on shorelines (emerging in the intertidal and supratidal zones) reduces salinity and therefore supports the presence of plant species with lower tolerance of saline soils, as well as increasing the productivity of plant communities. Where freshwater enters the intertidal (and supratidal) zone plant biomass may be higher, reflecting freshwater, sediment and other inputs that enhance plant growth and contribute to vertical accretion. In the wet tropics, freshwater is often abundant in the upper intertidal zone and communities can be mixed, comprised of mangrove species that have low tolerance of salinity and other tree species (e.g. *Melaleuca, Casuarina*) mixing with mangroves on the landward edge or ecotone (Bunt *et al.*, 1982). However, groundwater can also contribute to soils that are permanently flooded, which may reduce plant growth. In the arid and semi-arid regions of Australia, mangroves exhibit relatively low productivity (and biomass) and are restricted to areas where there is daily tidal inundation lower in the intertidal zone as they cannot physiologically withstand the hypersalinity (soil salinity more concentrated than seawater) that arises with limited tidal inundation. Saltmarshes and sparsely vegetated saltmarshes or saltflats typically occur in the high intertidal zones of arid and semi-arid regions where hypersaline conditions develop. In temperate regions, some sites have mangroves, while in cool climates mangroves are absent and saltmarsh communities dominate across the upper intertidal zone. Saltmarsh plant assemblages in southern Australia are particularly diverse and can have strong patterns in species distribution across the intertidal and supratidal zones that relate to patterns of inundation. Some species are woody (e.g. *Tecticornia arbuscula*) and reach shrub height and thus have higher levels of biomass.

Seagrass occurs below mean tide, both in the intertidal and sub-tidal zones. Seagrass biomass tends to be higher in regions with high light availability at the seafloor, and thus in Australia seagrass biomass and carbon stocks are higher in temperate and arid regions compared to the tropics and subtropics.

Coastal wetlands in different climatic regions achieve different levels of abatement (see Bunt *et al.*, 1982), and as such BlueCAMuses climatic region-specific rates of abatement by differing vegetation types and greenhouse gas emissions (see Table 4 and 9).

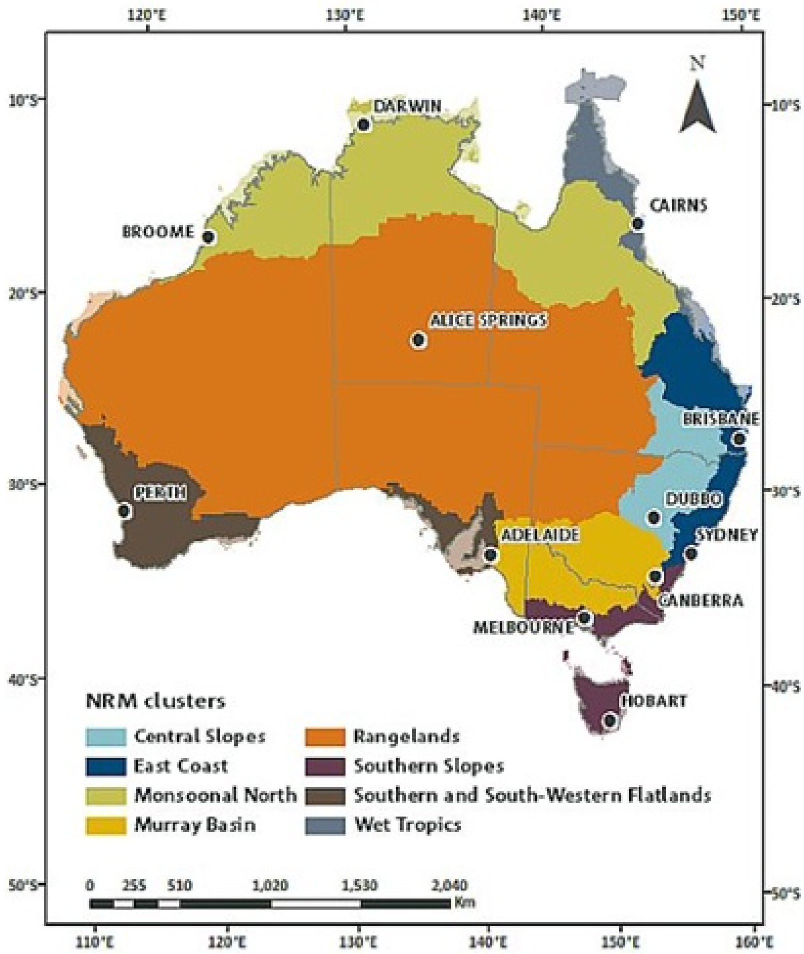

Figure 1: Variation in climate regions over Australia and associated Natural Resource Management clusters. In this document we use Tropical monsoon for “Monsoonal north”; Tropical humid for “Wet Tropics”; Subtropical for “East Coast”; Temperate for “Southern Slopes”, “Southern and South-Western Flatlands” and “Murray Basin” and Arid/Semiarid for “Rangelands” (Climate Change in Australia).

1.3 Variation in tidal range

1.3.1 General approach

Coastal wetland types, their productivity and soil carbon accumulation are influenced by tidal inundation. Tidal inundation at any particular site is influenced by tidal range and elevation of the land, which is expressed relative to the Australian Height Datum (AHD), where AHD = 0 is approximately mean sea level (MSL) , see Geoscience Australia’s website. Mangrove and/or saltmarsh typically occupy the upper half of the tidal range (Figure 2). Depending on climatic zones and local conditions, sparsely vegetated saltmarshes (saltflats) and/or supratidal forests (e.g. *Melaleuca* and *Casuarina* spp.) or other vegetation may occupy the supratidal zone. Seagrass typically occupy sub-tidal and lower intertidal (lower half of the tidal range) positions. Anticipated sea level rise will inundate land that is currently above the level of the highest astronomical tide (HAT) and thus projects should include (where possible) land that will be within the intertidal zone in 100 years (i.e. land that is within the elevation envelope of the HAT with anticipated levels of sea level rise).

This document describes and explains the tidal and land elevation parameters needed for reporting the Abatement Outcomes once the project is underway.

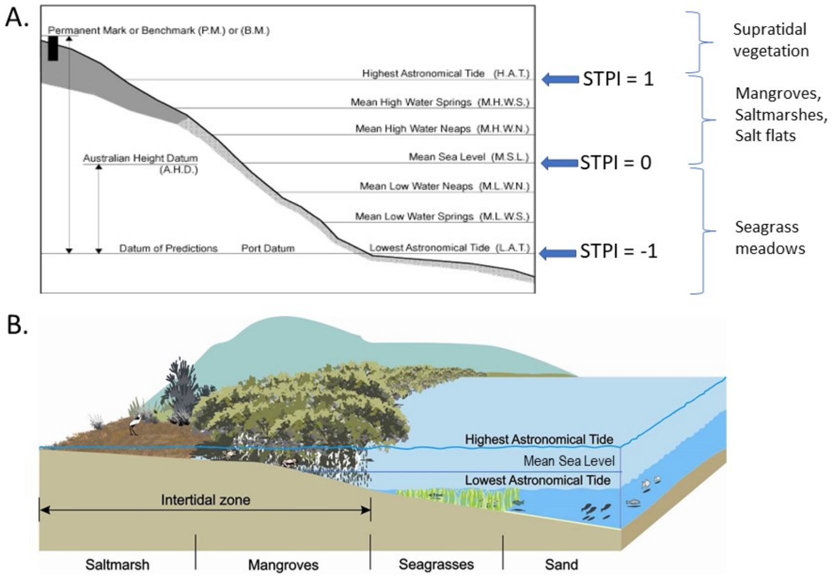

Figure 2: Tidal planes in semi-diurnal and diurnal tidal settings, the Standard Tidal Position Index (STPI) associated with tidal planes and the coastal wetland vegetation included within the tidal planes. The Australian Height Datum (AHD) is indicated. B. An example of coastal wetland types arranged across the intertidal zone and identification of important tidal planes (modified from Maritime Safety Queensland and Office of Environment and Heritage).

1.3.2 Tidal inundation and its influence on coastal wetlands

Levels of tidal inundation of the intertidal zone broadly follows elevation (or bathymetric – water depth, for seagrass) contours. Hence elevation may be used as a proxy to estimate types of coastal wetlands that will establish with introduction of tidal waters, and soil carbon sequestration across the intertidal zone. Elevation of the land relative to AHD can be used to stratify project sites into CEAs. For example, in Figure 2, saltmarsh occurs in the very upper part of the intertidal zone and mangroves occur in the middle part, above mean sea level, which would be designated as different CEAs.

As tides propagate through estuary entrances, along channels, into large open water bodies and across intertidal gradients they may become amplified or attenuated by site specific factors; this should be accounted for if possible as it will alter the elevation of tidal planes and thus vegetation types that develop at a local scale. See the Supplement for further detail.

- BlueCAM will require the area of different ecosystems that establish in order to estimate the abatement associated with those ecosystems over the duration of their growth. The ecosystems area will change over the lifetime of a project and thus adaptive project designs to capture changes may be needed.

1.3.3 Accommodating variation in tidal range around Australia in the model

Tidal range and tidal type (semi-diurnal or diurnal) vary around the Australian coast (Figure 3). Because of this variation, we express the elevation range of different coastal wetland communities as a proportion of the tidal range that could be occupied by particular coastal wetland types. This is determined as the proportion of the elevation between MSL to HAT and higher. Tidal range can be attenuated by barriers to tidal inundation, which can be natural or artificial and thus the tidal range should be measured as close to the project area as possible (see the Supplement).

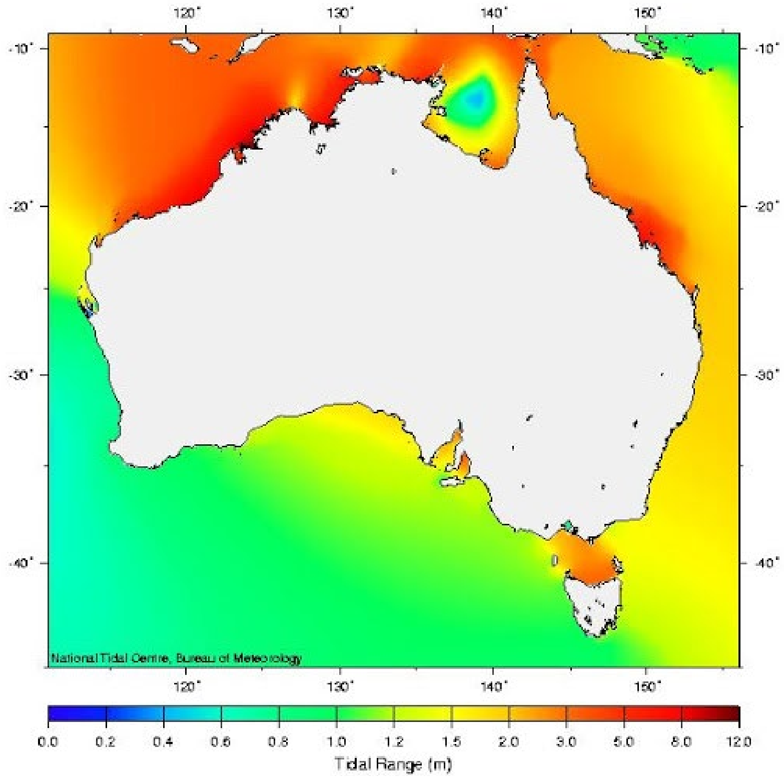

Figure 3: Variation in tidal range around Australia (Bureau of Meteorology, National Tidal Unit). Advice for stratification of sites to establish Carbon Estimation Areas

1.3.4 Delineating Carbon Estimation Areas (CEA)

Project areas may have different land-uses, vegetation types and levels of land elevation (relative to AHD) that can be used to delineate CEAs. Different CEAs need to be established for different land types within a project area. For example, CEA 1 may be ponds; CEA 2 may be freshwater wetlands on the lowest elevation land behind the tidal barrier; CEA 3 may be sparse woody *Melaleuca* on land with moderate elevation, and CEA 4 may be grazing land on the highest elevation land. If the project land has a homogenous land type (e.g. grazing land) in the baseline, prior to tidal introduction, which varies in elevation, then for each offsets report, different CEAs could be established based on elevation of the land and the coastal wetlands that have developed in the project area with tidal introduction.

The standardized tidal position index (STPI, adapted from Lal et al. 2020) is used to facilitate comparisons between different regions with different tidal ranges (i.e. tidal range is standardized to be between -1 for lowest astronomical tide and 1 for highest astronomical tide, with mean tide level being zero, see Figure 3).

$$STPI = (En – MTL)/(HAT – MTL); \qquad \textit{Equation 1}$$

where En is the upper or lower elevation boundary of the CEA (m above AHD, the local geodetic datum); MTL is the mean tide level (AHD, approximately mean sea level, MSL) and HAT is approximated by HHWSS or the high high-water solstices springs. The denominator in Equation 1 defines the upper half of the intertidal zone, which represents the vertical range that supports intertidal coastal wetlands and is expressed by the difference between HAT and MTL.

The presence of vegetation types and elevation ranges of different vegetation types vary among regions with climate (Table 2). For example:

- In subtropical and tropical monsoonal regions saltmarsh or mangroves may be present in the high intertidal zone, depending on groundwater availability and other factors.
- Tropical regions can either be in the monsoonal tropics where rainfall is highly seasonal or the wet tropics where rainfall is less seasonal.
- In temperate regions some locations have mangroves (e.g. Victoria) while others do not (Tasmania, parts of the south coast of Western Australia).

1.3.4.1 Flooded Land Carbon Estimation Areas

Methane and nitrous oxide emissions from flooded land

Drains, ditches, ponds and other constructed or managed water bodies can occur within project areas. These features can form flooded land CEAs and are allocated emission factors dependent on the land-use type and salinity of the water body.

- For Reporting the Abatement Outcomes, prior to tidal introduction water bodies may be 1) fresh or low salinity (<18 ppt, IPCC 2013) and have greenhouse gas emissions that will be avoided with tidal introduction (see Figure 7); or 2) saline (>18 ppt e.g. for aquaculture and salt production ponds) which have lower baseline GHG emissions.
- With the introduction of tides, emissions from ditches, drains, ponds, and other constructed water bodies are assumed similar to the coastal wetland vegetation with which they are associated.

1.3.5 Coastal wetland responses to sea level rise

Sea level rise is caused by ocean warming and melting of ice. The rate of sea level rise is temporally and spatially variable (Figure 4) with the projected rate accelerating toward the end of the 21st century. In response to sea level rise, coastal vegetation may move landward (sometimes called landward retreat or migration) as the tide reaches further inland and the supratidal areas become more frequently inundated by tides. In addition to landward migration of coastal wetlands, the levels of inundation will also increase over time. However, sediment delivery during tidal inundation and plant root growth result in vertical accretion and an increase in substrate elevations, which can reduce the impacts of sea level rise. However, increases in inundation may eventually drown coastal wetlands on the low elevation, seaward edges of the intertidal zone once the physiological and ecological tolerances of plant communities are exceeded.

Vertical accretion in wetland soils is important for soil carbon accumulation and for increasing elevation of wetland surfaces, which ultimately determines levels of wetland inundation with sea level rise. Rates of vertical accretion of sediments is typically higher in the lower intertidal zone than in the high intertidal zone, although rates may be variable in the low intertidal zone under dynamic hydrological conditions. The frequency and duration of inundation of wetlands can also be influenced by subsidence which can be caused by regional geological events, or from processes that typically affect the shallower layers of soil (soil volume) including compaction, bioturbation, decomposition of organic root material, declining groundwater levels or evaporation of soil water. High levels of subsidence (loss of elevation of land due to compaction) that are not compensated by high levels of vertical accretion essentially accelerate the rate of the sea level rise.

- When Reporting the Abatement Outcomes any effects of sea level rise on the project area will be incorporated in observed changes in the type and area of vegetation over time.

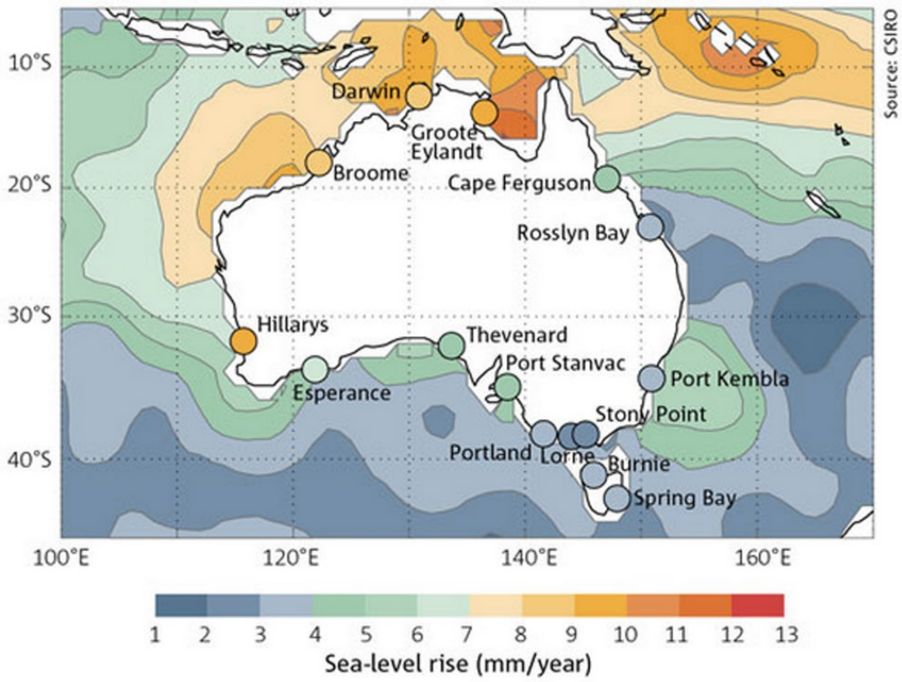

Figure 4: Sea-level rise rates around Australia, as measured by coastal tide gauges (circles) and satellite observations (contours) from January 1993 to December 2011 (CSIRO State of the Climate 2012).

1.3.6 Transitions among coastal wetland types with sea level rise and associated emissions

Over time, each CEA may transition to lower positions within the intertidal zone when vertical accretion is not sufficient to keep pace or exceed rates of sea level rise (Woodroffe *et al.*, 2016). In some cases, rates of vertical accretion are sufficient to balance or exceed rates of sea level rise (i.e. ecosystems “keep-up” with sea level rise and may extend their distribution laterally), but where rates of vertical accretion are low and the site is low in the intertidal then the saltmarsh or mangrove community may die and eventually be replaced by seagrass, unvegetated mud flats or other macrophytes (e.g. seaweeds or other aquatic plants) and CEAs must be designed to accommodate these vegetation transitions. Coastal wetlands will migrate to new areas higher on the shore as they adjust to sea level rise. If the elevation of any CEA (coastal wetland type) crosses its specified threshold of elevation with sea level rise, it will convert to the coastal wetland type typical for the new elevation CEA. This may include transitions to below mean sea-level where there is a possibility of seagrass colonisation (see below). For example, high intertidal zone saltmarsh CEA will transition to a mangrove ecosystem once the critical elevation threshold is crossed (as defined by the STPI ranges in Table 2). These ecosystem transitions can affect the abatement achieved over time. For example, in Figure 5, CEA 2 and 3 undergo transitions at 45 and 60 years respectively and both are associated with short-term (2-3 years) CO_2 emissions as biomass is decomposed.

For ecosystem transitions involving saltmarsh, seagrass and other herbaceous communities the original vegetation dies and biomass carbon will be assumed to have converted to CO_2 (emissions associated with ecosystem transitions, E_{TR}) and the new coastal wetland type will begin to accumulate biomass carbon at the rate specified for that wetland type for that climate region. For mangroves, CO_2 emissions do not occur with the transition from original scrub mangrove to taller mangroves as the same trees persist through the transition, increasing their growth rates. However, the death of mangroves (e.g. once they are lower than mean sea level), or death of supratidal forests, results in CO_2 emissions.

- When Reporting the Abatement Outcomes, E_{TR} from ecosystem transitions should be reported as 100% of the standing biomass of saltmarsh, seagrass or other herbaceous (non-woody) vegetation prior to the transition (see Table 5). For mangroves and supratidal forests and other woody vegetation, CO_2 emissions are calculated as 40% of the biomass (leaves, branches, fine wood and roots), assuming that wood of the trees (the bole) remains in place or decomposes very slowly, consistent with the IPCC 2019 guidance.

1.3.6.1 Transitions to seagrass – uncertainty and justification

For transitions when low intertidal mangrove or saltmarsh die because they are below the mean level of tides there is no strong basis to assume that the newly inundated habitat will necessarily support seagrass; sediment dynamics and propagule availability will likely determine whether seagrass will occur. However, as a general approach we assume that as sea level rise progresses, it will create potential habitat for seagrass. The extent and rate at which this will occur will vary in relation to the seagrass species present in adjacent areas and the stability of the newly formed shallow, subtidal habitat. In northern Australia, colonising genera such as *Halophila*, *Halodule* and *Zostera* are widely distributed and capable of rapidly colonising an area (Waycott et al. 2007). In temperate Australia, most tidal marsh habitat is in estuaries which typically support colonising seagrasses such as *Halophila*/*Ruppia* species (SW Australia) or *Zostera* (SE Australia) as well as the slow-growing, persistent species *Posidonia*. Assuming a nearby source of propagules, most of these genera (except for *Posidonia*) are likely to colonise new, suitable habitat within 2-3 years, as observed for colonising species of seagrasses in other locations where changes in sea level have created new habitat and conditions for plant establishment is suitable (Albert et al. 2017; Waycott et al. 2007) or predicted through modelling (Singer et al 2017). These genera (except for *Posidonia*) can occur in the lower intertidal zone, so there is no requirement for a particular water depth.

The extent of any new seagrass meadow will be limited by:
- the availability of soft sediment not occupied by the dead, remnant mangrove trees; and
- the stability of the sediment of the new habitat. Instability can prevent seagrass establishment through physical resuspension and through light limitation due to increased turbidity (Schumacher et al. 2014; Duarte 2007). The ongoing presence of dead mangrove trees may help to stabilise the sediments.
- If there is evidence that seagrass establishes as a result of the project, then BlueCAM can be used to calculate carbon accumulation in the area of seagrass at rates in Table 4 and Table (biomass and soils) for the particular climate region where the project is located.

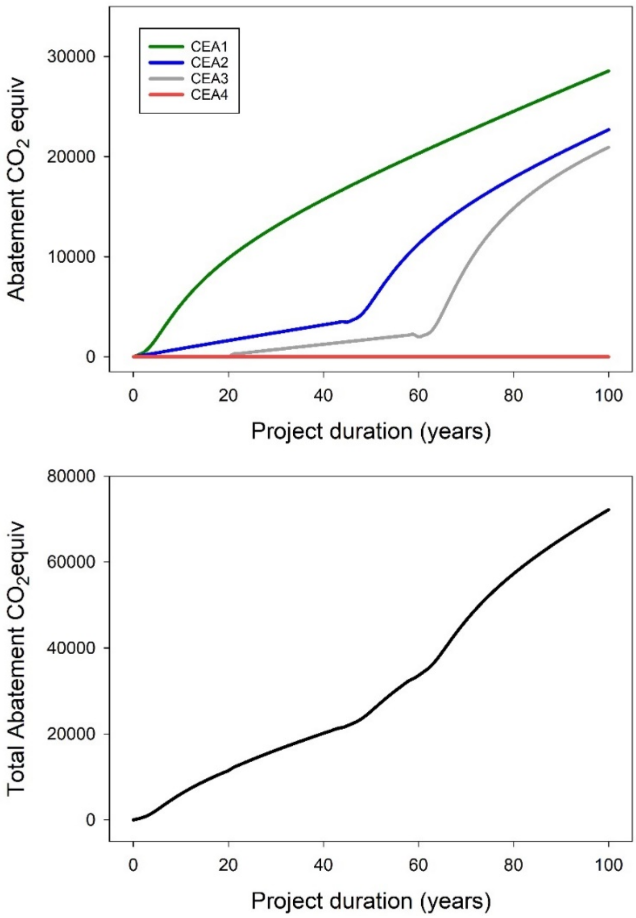

Figure 5: An example of estimated carbon accumulation in coastal wetlands for different CEAs (at different elevations) and with sea level rise. Carbon abatement in four CEAs is shown in the upper panel. Inflections in the blue and grey lines indicate when elevation thresholds for ecosystems are crossed, living biomass is decomposed and emitted as CO_2 in one year, and carbon accumulation changes to that of the new vegetation type. The lower panel shows total abatement in the site (101 ha) over the 100-year permanence period.

1.4 Estimation of biomass carbon

1.4.1 Aboveground Biomass – General approach

The general approach to estimating abatement in biomass accumulation in woody communities (mangroves and supratidal forests) is similar to other Emissions Reduction Fund (ERF) methods, where biomass accumulation is modelled using a standard curve that reaches a plateau level (mature standing biomass C) when the vegetation is mature. The form of the curve is based on empirical observations (Table 4) and the mature aboveground biomass based on the mean of field observations for each climatic region. Belowground biomass is modelled as a fixed proportion of aboveground biomass, reflecting the median value derived from empirical data (see 1.5.2). We use the median value because the median is less sensitive to observations in the data set that are very high and therefore provides an accurate estimate compared to use of the mean value (i.e. use of mean values may over-credit).

Mangroves and supratidal swamp forests have woody biomass that is generally higher per hectare in tropical and subtropical regions than temperate and arid regions. Mature biomass of mangrove stands is also higher lower in the intertidal zone (closer to the shoreline), compared to higher in the intertidal zone and a multiplier is applied to reduce the aboveground biomass in mangroves higher in the intertidal zone. The multiplier used is based on the STPI of the CEA, where the STPI of the CEA is calculated from the mean land elevation of the CEA (elevation relative to AHD) and the site specific tidal range data (provided by the project) (Table 2). The multipliers in Table 2 are based on observations from case studies around Australia that show that carbon accumulation in biomass and soils in the high intertidal zone, where tidal inundation is less frequent, is lower than that in the low intertidal zones where tidal inundation is more frequent. For example, in the arid/semi-arid regions mature biomass scrub mangrove will be half of the regional value provided in Table 4. The application of multipliers reduces the total abatement that is credited (compared to use of a single regional value) and therefore reduces the chance of over estimating abatement.

Saltmarsh and seagrass have lower aboveground biomass compared to mangroves and supratidal swamp forests. After restoration it is assumed that biomass is accumulated within 1 year. This may take longer in temperate and arid/semi-arid regions with woody saltmarsh species, although currently there is insufficient data to inform the use of a growth curve to achieving mature biomass.

Table 2 The elevation ranges of CEAs using the STPI for each defined climate zone and vegetation type used to estimate aboveground biomass (model/default value), and the multiplier to estimate the proportion of mature biomass (biomass factor "a" in Eq 2, see Table 4) and to use in estimating biomass accumulation and soil carbon sequestration and in higher elevation CEAs. In subtropical and tropical monsoon regions, the high intertidal may be occupied by mangroves or saltmarsh, depending on local conditions. In tropical regions, mangroves occupy more of the intertidal zone (i.e. Tropical-humid) compared to the monsoonal tropics, which are typical of the north coast of Australia. Mangroves are present in some temperate regions but not others.

Vegetation type	STPI range of Carbon Estimation Area (CEA)	Model / default value to use	Multiplier - Aboveground biomass	Multiplier - Soil carbon
Arid – semi-arid				
Seagrass	< 0	seagrass	1	1
Tall mangrove	0 - 0.40	mangrove	1	1
Scrub mangrove	0.40 - 0.47	mangrove	0.5	0.5
Sparsely vegetated saltmarsh (saltflat)	0.47 - 1.0	sparsely vegetated saltmarsh (saltflat)	0	1
Saltmarsh	0.47 - 1.0	saltmarsh	1	1
Supra-tidal	>1	supratidal (non-forested)	No data	No data
Subtropical				
Seagrass	< 0	seagrass	1	1
Tall mangrove	0 - 0.37	mangrove	1	1
Scrub mangrove	0.37 - 0.73	mangrove	0.75	0.5
Tall hinterland mangrove (if present)	0.73 - 1.0	mangrove	0.9	0.35
Saltmarsh (if present)	0.73 - 1.0	saltmarsh	1	1
Supra-tidal	>1	supra-tidal (forested)	1	1
Tropical - monsoon				

Vegetation type	STPI range of Carbon Estimation Area (CEA)	Model / default value to use	Multiplier - Aboveground biomass	Multiplier - Soil carbon
Seagrass	<0.1	seagrass	1	1
Tall mangrove	0 - 0.49	mangrove	1	1
Scrub mangrove	0.49 - 0.68	mangrove	0.35	0.50
Salt flat	0.68 - 0.81	sparsely vegetated saltmarsh (saltflat)	0	1
Tall hinterland mangrove (if present)	0.81 - 1.0	mangrove	0.35	0.35
Saltmarsh (if present)	0.81 - 1.0	saltmarsh	1	1
Supra-tidal zone	>1	supratidal (forested)	1	1
Tropical - humid				
Seagrass	< 0	seagrass	1	1
Tall mangrove	0 - 0.32	mangrove	1	1
Scrub mangrove	0.32 - 1.0	mangrove	0.7	0.7
Supra-tidal	>1	supratidal (forested)	1	1
Temperate – with mangroves				
Seagrass	<0	seagrass	1	1
Mangrove	0 - 0.45	mangrove	1	1
Saltmarsh	0.45 - 1	saltmarsh	1	1
Supra-tidal	>1	supratidal (forested)	1	1
Temperate – no mangroves				
Seagrass	<0	seagrass	1	1
Saltmarsh	0 - 1	saltmarsh	1	1
Supra-tidal	>1	supratidal (forested)	1	1

1.4.1.1 Estimating biomass under baseline scenarios

Woody biomass in the baseline (either unmanaged forests or *Melaleuca* forests) is assumed to be sparse woody vegetation that has grown recently on land initially cleared for agriculture (cropping or grazing). In the model, biomass of this vegetation was estimated to be similar to a mixed species planting stand that is approximately 15 to 20 years old, or 60 Mg dry matter ha^{-1} (Paul et al. 2015). In many cases vegetation will be younger than 15-20 years as woody vegetation is regularly cleared by landholders for grazing or other agricultural land-uses. Thus, this assumption results in lower estimates of abatement as the emissions resulting from a loss of woody vegetation caused by project activities may be overestimated. The biomass of herbaceous vegetation in the baseline is assumed to be 4.2 Mg dry matter ha^{-1} (National Inventory Report Volume 2, Australian Government Department of Industry, Science, Energy and Resources).

1.4.1.2 Mangrove aboveground biomass

Mangroves are comprised of woody vegetation that have similar characteristics to terrestrial woody vegetation and therefore the process to estimate accumulation of biomass carbon is similar to that used for woody vegetation in FullCAM. To establish the rate of mangrove aboveground biomass accumulation over time for abatement estimates, examples of mangrove aboveground biomass carbon development were sourced from published and unpublished studies (Sasmito et al. 2019, Kandasamy et al. 2021, Table 2.3). Mangrove tree yield curves were of the form typical for woody vegetation:

$$AGB = a*(exp(-k/age)) \quad \textit{Equation 2}$$

where "*a*" approximates the mature above ground biomass and "*k*" the rate of biomass increase over time (Paul *et al.*, 2015; Preece et al. 2017).

Nine global data sets, where the trajectory of mangrove growth has been quantitatively described, were used to establish the slope ("k") of the growth curve, which describes the rate of biomass increase in mangrove stands over time. We used global data, in addition to data available in Australia, to increase the size of the data set for analysis and to provide growth curves from a range of climatic settings. The mean "k" for these nine mangrove growth chronosequences was 29.6 with standard deviation of 29.7 (

Table 3). The mean value of “k” is higher than that of mangrove plantations (“k” = 13) and also of values typically used to describe regrowth of terrestrial woody vegetation in Australia (“k” = 15.7, Preece et al. 2017), indicating comparatively slower rates of biomass increase, which leads to estimates of abatement that are less likely to over estimate abatement.

Mean mature aboveground biomass carbon (“a”) for the climatic regions in Australia are listed in Table 4 (see the case study in Appendix 2.2). Using mean values of mature biomass results in accurate project-level estimates of abatement as mean values are less (approximately half) than the maximum biomass carbon that could be achieved in each climatic region. Analysis of mangrove stand biomass data in Australia found biomass to be similar in humid and monsoonal tropics and thus a similar value of mature biomass was used in both climate regions. Data from arid and semi-arid regions were combined to provide one value of mature mangrove biomass value for these regions that are similar to that for temperate regions and less than half of that observed in tropical regions.

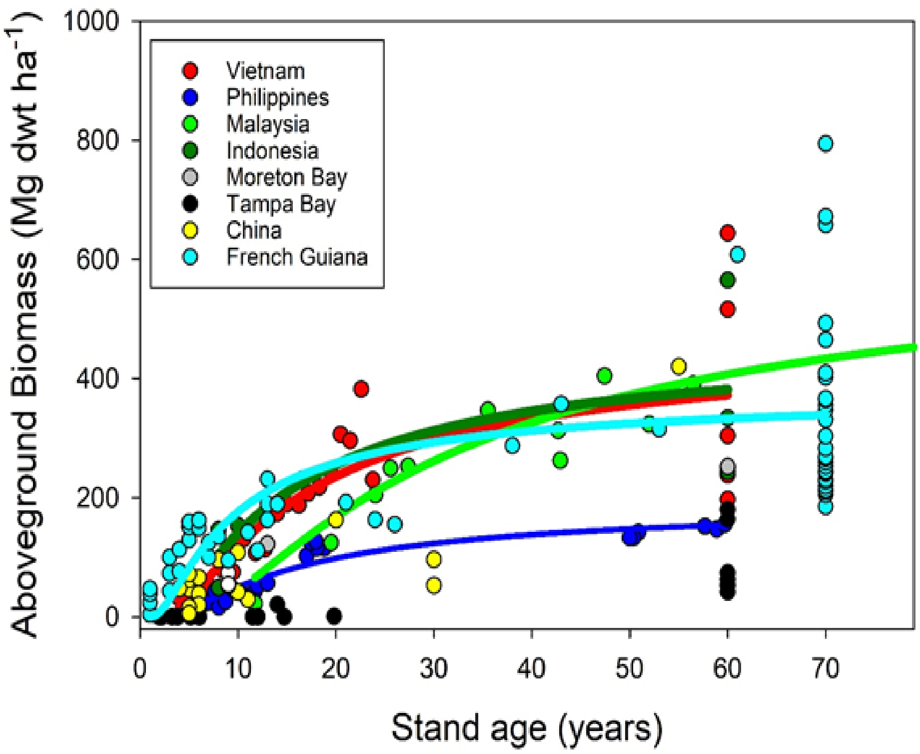

Figure 6: Examples of variation in mangrove aboveground biomass (Mg dry weight ha^{-1}) over stands of different ages. Data are from eight sites; Vietnam (red), Philippines (dark blue), Malaysia (light green), Indonesia (dark green), Moreton Bay, Australia (grey), Tampa Bay, Florida, USA (black), China (yellow), French Guiana (light blue). Natural sites are those equal to or greater than 60 years. Curves are fitted where there was sufficient data, including Vietnam (red), Philippines (dark blue), Malaysia (light green), Indonesia (dark green) and French Guiana (light blue). Curve parameters are represented in Table 2.

Table 3 Parameters for biomass accumulation curves of mangroves from mangroves. The curves are of the form AGB (Mg dwt ha-1) = a(exp(-k/age)), where "a" approximates the mature above ground biomass and "k" the rate of biomass increase over time. Mean "k" is 29.6 with standard deviation of 29.7 (standard error 9.9).*

Location	Species	Activity	a	k	R^2	Reference
Vietnam	*Rhizophora apiculata*	Plantation	467.6 ± 61.5	13.69 ± 3.09	0.632	Phan et al. 2019
Philippines	*Rhizophora apiculata*	Plantation	193.3 ± 11.9	13.49 ± 1.33	0.895	Salmo et al. 2013
Malaysia	*Rhizophora apiculata*	Plantation	604.4 ± 53.5	13.12 ± 2.36	0.817	Adame et al. 2018
Indonesia (Bali)	*Rhizophora apiculata*	Planted shrimp ponds	465.7 ± 111.6	11.99 ± 6.40	0.642	Sidik et al. 2019
French Guiana	*Avicennia germinans*	Natural regeneration	377.7 ± 27.7	7.61 ± 1.98	0.484	Walcker et al. 2018
India	*Avicennia marina*	Planting mud flats	621.5 ± 308[a]	58.1 ± 11.9	0.721	Kandasamy et al. 2021
Indonesia (Papua)	*Rhizophora apiculata*	Natural regeneration	464.6 ± 26.2	26.4 ± 1.74	0.990	Sillanpaa et al. 2016
Australia (NSW)	*Avicennia marina*	Natural regeneration	405.7 ± 27.7	97.8 ± 25.6	0.696	Unpublished
Australia (SA)	*Avicennia marina*	Natural regeneration	171.5 ± 24.9	23.9 ± 6.7	0.383	Unpublished

Footnote: [a] No data for older (>27 year) stands provided.

1.4.1.3 Biomass of supratidal swamp forests

To estimate biomass of mature supratidal forests, data were compiled from six studies that included biomass of *Melaleuca* spp. forest from the Northern Territory, tropical and subtropical QLD, and for *Casuarina* stands for NSW and WA, which represent the range of forest structure likely to occur over Australia - to estimate mature biomass for supratidal forests in different climate regions (parameter "a"). Supratidal forests from arid and semi-arid zones were not represented in the data, but estimates based on forest structure of *Melaleuca* stands in South Australia were similar to those of subtropics and thus subtropical values which are low compared to tropical and temperate regions were applied in arid and semi-arid regions that are consistent with known variation in biomass over variation in rainfall and temperature. While mature aboveground biomass was derived from field data (Table 3), estimates of growth rates of supratidal forest stands were modelled using a standard approach for other forests, given the similarity in growth among tree species observed in experimental plots (Preece et al. 2017). To estimate biomass accumulation of supratidal forest stands that develop within the project area, increases in aboveground biomass carbon over time used the same modelling approach as for mangroves and used for other species (Paul et al. 2015), where biomass increases to a maximum at maturity ("a"). The rate of increase of biomass for supratidal forest trees ("k") was assumed to be similar to that described for mangroves ("k" = 29.6) and with similar allocation to belowground biomass (Table 4). As described above, the value of "k" describes slow growth (compared to that for other dryland trees, Paul et al. 2015) and therefore results in estimates of abatement that are less likely to overestimate abatement.

1.4.1.4 Saltmarsh and seagrass aboveground biomass

Saltmarsh and seagrass biomass varies among species assemblages, and may be dependent upon local hydrological conditions (e.g. freshwater inputs, depth) and larger-scale climatic and oceanic drivers. Saltmarsh biomass estimates were not provided for all climate regions as in most climate regions saltmarsh vegetation is comprised of herbaceous vegetation with relatively low biomass (Serrano et al. 2019). Therefore, similar estimates of aboveground biomass of saltmarsh were applied to subtropical zones, tropical and arid/semi-arid zones. A higher value of saltmarsh biomass was used for temperate zones where woody saltmarsh species commonly occur (Table 4).

Seagrass communities may have lower biomass in tropical and subtropical settings than in temperate settings and arid/semiarid settings (with the exception of tropical species from the genera Enhalus and Thalassia), reflecting variation in species composition in response to variation in temperature and light at the benthos and herbivory. Light levels at the benthos are typically higher in temperate and arid/semiarid settings due to lower levels of turbidity associated with river flows. Additionally, some regions and habitats have seagrass communities comprised of long-lived, larger seagrass species. Because of these regional differences in environmental conditions and seagrass species composition, similar seagrass biomass estimates were applied to tropical and subtropical settings, with higher values of seagrass biomass applied to temperate and arid/semi-arid regions (Table 4).

Sparsely vegetated saltmarsh will occupy some upper intertidal elevations and maybe covered with cyanobacterial mats - in these settings biomass carbon is set to zero.

1.4.2 Belowground biomass

In all coastal wetlands fine roots (both living and dead) are included in the belowground carbon pool. In the model it is assumed that fine roots are incorporated in the soil organic carbon stocks reflecting common field and laboratory approaches to measuring wetland soil carbon, and thus only larger roots (> 2 mm) are included in the belowground biomass estimates.

For saltmarsh and seagrass, a high proportion of the root biomass is fine roots (< 2 mm), concentrated within the surface ~20 cm of the substrate. This root biomass is included within the soil carbon accumulation estimates (see 1.5), and therefore belowground biomass for saltmarsh and seagrass is set to zero.

In mangroves the proportion of aboveground to belowground biomass (root shoot ratio, R:S) was obtained from eight studies in Australia that included sites from the Northern Territory, tropical and subtropical Queensland, NSW, arid WA and SA. Root biomass was extrapolated to one meter depth accounting for the fact that 75% of the roots are located in the top 45 cm (Castaneda-Moya et al. 2011). R:S tends to be higher when the forest is dense, which is a characteristic of young forest. As the forest matures R:S will decrease. It is assumed that over the reporting period (25 years) the forest will have matured and the R:S value will be an average of young and mature forests. Best estimate for R:S is 0.32 (median), 0.47 (average), 0.07 (standard error) confidence interval around the median at 95% of 0.17 to 0.47. For supratidal forest a R:S value of 0.27 is used based on values reported for tropical trees Mokany et al. (2006).

Table 4 Mean mature (± 1 standard deviation) aboveground biomass carbon (Mg C ha^{-1}), parameter "a" in equation 2 for coastal wetland vegetation in Australia in different climatic regions from Serrano et al. (2019). Carbon stocks in supratidal swamp forest (Mg C ha^{-1}) are obtained from 6 Australian studies (Adame et al. 2019). N is the number of sites.

Climatic region	Mangrove	Saltmarsh	Supratidal Swamp forest	Seagrass
Tropical (humid and monsoon)	167 ± 101 (N = 15)	Use subtropical	192 ± 55 (N = 6)	0.20 ± 0.19 (N=391)
Subtropical	101 ± 78 (N = 5)	1.36 ± 0.37 (N = 3)	100 ± 34 (N = 3)	Use tropical
Semi-arid	70.3 ± 41 (N = 8)	Use subtropical	Use subtropical	Use tropical
Arid	Use semi-arid	Use subtropical	Use subtropical	Use Temperate
Temperate	70.4 ± 41 (N = 9)	7.89 ± 6.08 (N =49)	178 ± 41	0.57 ± 0.66 (N=74)

1.4.3 Approach for adjusting mangrove biomass for environmental gradients over the intertidal zone

Mangrove biomass varies over the intertidal zone, with higher biomass lower in the intertidal zone than the upper intertidal zone, where scrub forms of mangrove species occur. Scrub mangroves can be 15 to 50% of the biomass of taller forests, the proportion varying among climatic regions (Table 1). To reflect the lower biomass of scrub mangroves in higher elevation areas a multiplier is applied to the mature mangrove biomass for calculation of biomass carbon accumulation over time. The multiplier used is based on the STPI of the CEA, where the STPI of the CEA is calculated from the mean land elevation of the CEA (elevation relative to AHD) and the site specific tidal range data (provided by the project) (Table 2). The multipliers in Table 2 are based on observations from case studies around Australia that show that carbon accumulation in biomass and soils in the high intertidal zone, where tidal inundation is less frequent, is lower than that in the low intertidal zones where tidal inundation is more frequent. For example, in the arid/semi-arid regions mature biomass in the high intertidal zone will be half of the regional value provided in Table 4. The application of multipliers reduces the total abatement that is credited (compared to use of a single regional value).

1.5 Estimation of soil carbon accumulation in baseline and project scenarios

1.5.1 General approach

Carbon stored in wetland soil constitutes a significant carbon pool in most wetland ecosystems (Duarte et al., 2013). The saturated nature of wetland substrates slows the decomposition of belowground carbon, meaning a proportion of this carbon pool may remain sequestered within the substrate over centennial to millennial timescales (Rogers et al., 2019). The majority of new carbon inputs to the substrate are lost over shorter time frames (days to decades) to the atmosphere as CO_2 or CH_4 through decomposition processes or to other ecosystems through lateral flux of particulate, dissolved, and gaseous C (Alongi, 2014). Measurement of carbon accumulation rate (CAR) – typically calculated through radiometric dating of substrates, monitoring of surface elevation table – marker horizon (SET-MH) benchmarks, and/or a repeated measures approach (i.e. stock difference) – are widely used to estimate change in soil carbon pools through time (see case study in Appendix 2.2).

1.5.2 Estimating soil carbon accumulation under baseline scenarios

Soil carbon dynamics are likely to vary depending upon the specific conditions of a baseline setting. That is, CAR in the baseline scenario may be negative (i.e. a net emission of CO_2 from the substrate) or positive (i.e. substrate acts as a net sink of CO_2). A shift in land-use from baseline scenarios where soil organic matter is oxidised due to drainage, disturbance or excavation of substrates, to one in which it does not occur can be a significant CO_2 abatement benefit of some restoration projects (Needelman et al., 2018). Decomposition dynamics largely control the direction and magnitude of fluxes and are influenced in part by changes in inundation/moisture, temperature regimes as well as the amount of soil disturbance resulting from the baseline activity.

Assessment of available published and unpublished data from locations subject to tidal-restriction was used to estimate soil carbon accumulation in baseline land-uses relevant to tidal restoration projects in Australia. There are IPCC Tier 2 estimation approaches for some - but not all - baseline, land-uses (Hagger et al., 2021, in press). Tidally-restricted wetlands may accumulate some soil carbon (Fennessy et al., 2019), and this is quantified for Australian settings (Table 9 in Appendix 2).

Based upon variations in the availability and suitability of existing data among different baseline land-uses, two accounting approaches are outlined for the estimation of soil CAR in baseline scenarios.

1.5.2.1 Default carbon accumulation rate values / emission factors

For a subset of baseline land uses, data are available to generate default values of soil CAR under the baseline scenario (
Table 5). Land uses include salt evaporation ponds (for which multiple studies have demonstrated no soil carbon accumulation); sparsely vegetated hypersaline saltmarsh (or high intertidal saltflats), and tidally-restricted wetlands (where tides have been prevented from entering the land by structures that moderate tidal water flows). For tidally-restricted wetlands, the value is derived from estimates of soil CAR in hydrologically disturbed mangrove, saltmarsh, and herbaceous settings, and is therefore applicable to a range of baseline wetland scenarios.

For land-uses where net emission of soil CO_2 can be assumed, but there is insufficient data to support an emission factor, baseline CAR can be set to zero, i.e. where IPCC stock change factors land use (F_{LU}), input (F_I) and management (F_{MG}) have a value < 0 (see Table 6). In these cases, avoided emissions from soils in the project area are zero.

Table 5 Default values for soil CAR under specific baseline land uses

Baseline land-use	Default value CAR (Mg C ha^{-1} yr^{-1})	References
Salt evaporation pond	0	(Gulliver et al., 2020; Mosely et al., unpublished data)

Sparsely vegetated hypersaline saltmarsh (saltflats)	0.25	(Brown et al., 2021) Project default value
Tidally-restricted wetland (freshwater or brackish)	0.47	(Kelleway et al. unpublished data; Jones, Lavery et al. unpublished data)
Supratidal forest	0.61	Project default value
***Land uses with default stock change multiplier < 0**	0	IPCC 2019

* See IPCC default stock change factors section 1.6.2.2 below

1.5.2.2 Soil carbon loss with agricultural processes using IPCC default stock change factors

This approach utilises default stock change factors described in the 2019 Refinement to the 2006 IPCC Guidelines for National Greenhouse Gas Inventories. Under this approach, default stock change factors are applied for three parameters: land use (F_{LU}), input (F_I) and management (F_{MG}) (Equation 3). Use of IPCC default stock change factors has been used for a subset of land uses amenable to tidal restoration projects in the wet tropics of Queensland (Hagger et al, 2021) (
Table 6), though this is amenable to project-specific application over a broad range of land uses and climate zones.

Following Hagger et al, (2021), this approach uses the national FullCAM soil carbon map (Viscarra Rossel et al., 2014) to derive activity-specific soil organic carbon stock estimates. A series of stock change factors specific to land use type and intensity (i.e. $F_{LU;}$ $F_{I;}$ and F_{MG}) in the baseline scenario are applied to site-specific soil carbon stock data to estimate the annual change in the baseline soil carbon pool over a 20 year period:

For calculation of baseline soil CAR per unit of area (i.e. Mg C ha^{-1} yr^{-1}) assuming a global warming potential (GWP) of 1:

$$\text{CAR} \ (Mg \ \text{C ha}^{-1} \ yr^{-1}) = (SOC\ stock\ (Mg \ \text{C ha}^{-1}) - (SOC\ stock\ (Mg \ \text{C ha}^{-1}) \times F_{LU} \times F_{MG} \times F_I)/20)) \qquad \text{Equation 3}$$

Table 6 Summary of default stocks change parameters for a subset of baseline land uses in tropical Queensland. Where land use (F_{LU}), input (F_I) and management (F_{MG}) are provided. Default stock change multiplier is the product of (F_{LU} x F_I x F_{MG})/20 (IPCC 2019)

Baseline land-use	Default stock change multiplier (product of F_{LU} x F_I x F_{MG})	F_{LU}	F_I	F_{MG}
Agriculture: cropping: sugarcane	0.61	0.48 (Long-term cultivated, tropical, moist/wet)	1.15 (High tillage without manure, tropical, moist/wet)	1.11 (Reduced tillage, tropical, moist/wet)
Agriculture: grazing	0.97	1 (Permanent grassland)	1 (No additional improvements	0.97 (Tropical moderately degraded grassland)

Mean values of SOC for grazing and sugarcane (cropping) land for Australia are derived from the Australian soil carbon map (Viscarra Rossel et al. 2014) for land on the coast (delineated using the Smartline Coasts Sediment Compartment and Realms data, available online) (Table 7). Soil carbon stocks in ponds and drainage channels and ditches can be assumed to be similar to the surrounding land-use.

Table 7 Mean values of SOC stocks to 30 cm for grazing and sugarcane (cropping) land for Australia. Values are derived from the Australian soil carbon map (Viscarra Rossel et al. 2014) for land on the coast (delineated using the Smartline Coasts Sediment Compartment and Realms data, available online). NA indicates where data is not available.

Climatic region	Grazing	Sugarcane
Tropical monsoon	40.2	42.0
Tropical humid	63.7	67.8
Subtropical	65.3	64.0
Semi-arid/Arid	30.4	NA
Temperate	62.2	NA

Stratification of CEAs for baseline scenarios

If multiple baseline land-uses exist within the project area, then baseline-scenario stratification will be required. If using IPCC default stock change factors then any variations in land use, inputs and management (i.e. F_{LU} or F_I or F_{MG}) would require delineation into separate carbon estimation areas based upon differences in these parameters.

1.5.3 Estimating soil carbon accumulation under tidal introduction project scenarios

1.5.3.1 General approach

The approach for estimating change in soil carbon stocks in project scenarios is similar to other guidance and methods (i.e. IPCC, VCS), in that default values of carbon accumulation rate (CAR) have been derived on the basis of the best available data. Estimates are based upon a national collation of blue carbon (Serrano et al., 2019) updated to include recently published and unpublished datasets. Default values for soil carbon accumulation are disaggregated based upon differences among ecosystem types (Table 8; Figure 7). Within each ecosystem type there were no significant differences in CAR among climatic zones (P>0.05) (See Appendix 3 Figure 15 and Figure 16 for comparison of soil carbon stocks). There are no significant differences in CAR among saltmarshes that differ in herbaceous structure (succulents, grasses; typically occupying lower saltmarsh elevations) compared to rush-dominated saltmarshes (typically occupying higher intertidal elevations) and thus a single value of soil carbon accumulation is applied for all saltmarsh types, but a lower value for sparsely vegetated saltmarsh (saltflats).

Table 8 Summary of data of available published and unpublished carbon accumulation rate (CAR) estimates by ecosystem

Ecosystem	Number of estimates (n)	CAR (Mg C ha^{-1} yr^{-1})				
		Mean ± 1SE	Median	95%CI lower	95% CI upper	Default Value
Seagrass	43	0.32 ± 0.05	0.21	0.23	0.42	0.21
Mangrove	48	1.40 ± 0.16	0.95	1.07	1.73	0.95
Saltmarsh	28	0.77 ± 0.22	0.48	0.32	1.21	0.48
Supratidal forests	8	0.62 ± 0.05	0.61	0.51	0.74	0.61
Sparsely vegetated saltmarsh (saltflat)	3	0.23 ± 0.06	0.25	0	0.49	0.25

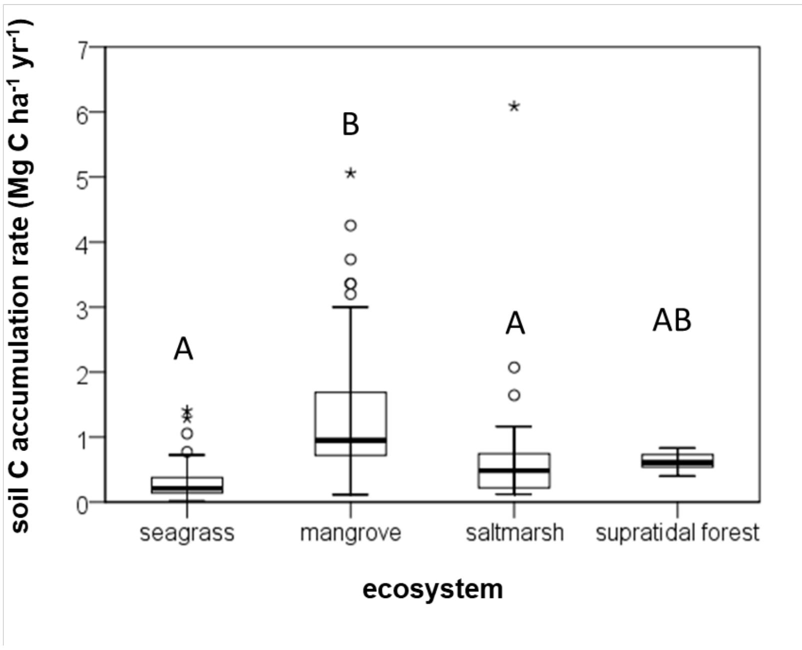

Figure 7: Box and whisker plot of Australian soil carbon accumulation rates by ecosystem type.. Solid horizontal lines within each box represent the median estimate. Stars and circles represent extreme values and potential outliers respectively.

The following steps were followed in deriving ecosystem soil carbon accumulation rates to ensure estimates of abatement are accurate for Australian settings:

1. Only data derived from Australian sites are included in the calculation of soil carbon accumulation values, as Australian coastal wetlands typically accumulate and preserve soil carbon at rates lower than global averages (Duarte et al., 2013; Rogers et al., 2019; Serrano et al., 2019). Default values for Australia (Table 8) are lower relative to both IPCC emission factors and the combined default value

for mangrove and tidal marshes under VCS method VM0033 (i.e. 1.63 Mg C ha yr^{-1}) (Needelman et al., 2018).

2. In the absence of sufficient data specific to restored wetlands, estimates from natural (undisturbed) wetlands are used. Comparison of soil carbon accumulation in restoration scenarios against natural wetlands shows this to be a suitable approach for mangrove (Appendix 3 Table 13) and saltmarsh (Appendix 3 Table 13). Published and unpublished post-restoration (tidal restoration) data exist and are included in the calculation of project default soil accumulation values.

3. Median values are applied to ensure an accurate project-level approach, relative to the use of mean values, thereby reducing the influence of extremely high or low estimates in the datasets.

1.5.3.2 Contributions to soil carbon

Soil and sediment (hereafter "soil") can accumulate C through autochthonous (internal) or allochthonous (external) inputs. Autochthonous inputs include:
(1) Surficial inputs from vegetative aboveground litter production that are incorporated into soils; and
(2) Belowground inputs from production of roots and rhizomes.

In herbaceous wetlands (e.g. saltmarsh), this belowground production tends to be concentrated in in the upper ~20 cm of the substrate. In some cases – particularly forested wetlands including mangrove - contemporary root growth may also occur at depths of up a metre or more below the surface (e.g. Kelleway et al., 2017), and can constitute a major source of carbon accumulation (Lamont et al., 2019). This presents a major challenge to the accurate determination of soil carbon accumulation rate.

The median values calculated for soil carbon accumulation are based upon methods which capture accumulation near the soil surface, but do not account for root growth deeper in the soil. The estimation of belowground biomass using a ratio to aboveground biomass is applied for forested ecosystems (mangrove and supratidal forest) to include root growth of these ecosystems (see section 1.5.2). For saltmarsh and seagrass, root growth deeper in the soil profile is assumed to be zero, so no belowground biomass factor is applied.

For further detail, see guide to biomass estimation (see 1.5.2).

1.5.3.3 Adjustment of CAR for variation over intertidal gradients

Project-scenario stratification for soil CAR follows the general approach of adjusting the biomass carbon pool (see section 1.5). That is, for each climatic zone strata are defined based on position within the tidal frame. This approach fits with models of soil carbon accumulation in tidal wetlands. First, soil CAR is influenced by belowground biomass productivity (Lamont et al., 2019). Second, locations situated lower in the tidal frame with more vertical available accommodation space, because of greater depths of inundation, tend to accumulate carbon at higher rates than locations situated higher in the tidal frame due to sediment trapping and enhanced root production (Kirwan and Megonigal, 2013; Rogers et al., 2019).

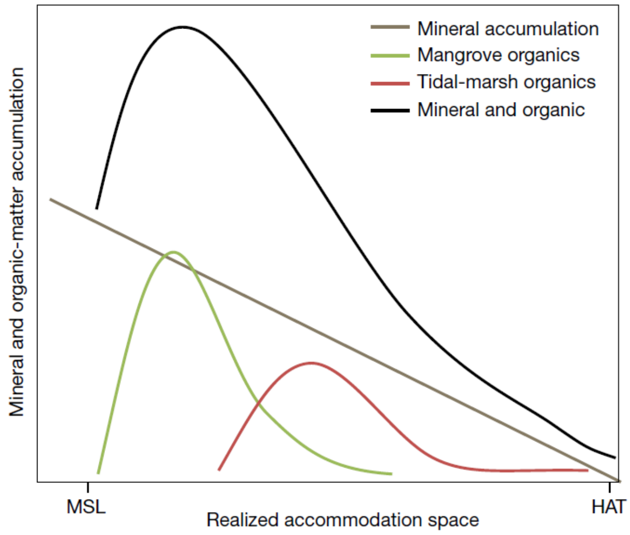

Figure 8: Conceptual links between mineral and organic-matter accumulation and realized accommodation space (Source: Rogers et al. 2019, adapted from Kirwan & Megonigal 2013). MSL = Mean Sea Level and HAT = Highest Astronomical Tide.

For mangroves, tall mangroves located in the lower half of the upper intertidal zone (Standard Tidal Position Index from 0 to 0.5) are applied a soil carbon accumulation multiplier of one (i.e. the default value). For other mangroves at higher in the intertidal zone, a multiplier equivalent to the decline in the aboveground biomass at positions higher compared to lower in the intertidal zone is applied (e.g. a soil carbon multiplier value of 0.5 reduces soil carbon accumulation by 50% in the high intertidal zones compared to lower intertidal zones) (Table 2).

A soil carbon accumulation multiplier of one (i.e. the default value) is applied for all saltmarsh as patterns of CAR variation at different tidal position are assumed offset by the presence of higher biomass assemblages (i.e. rushes or woody shrubs) at high elevations. This is reflected in the lack of difference in CAR between herbaceous and rush-dominated saltmarsh assemblages. Multipliers are based on known lower rates of soil carbon accumulation in the high compared to the low intertidal zone in Australian and internationally.

For seagrass and supratidal forests there are either no clear patterns of spatial variation, or too few data to support differentiation of soil CAR by stratification. All locations will therefore apply the ecosystem-specific median estimate default value. For further detail see Table 2.

1.6 Estimation of greenhouse gas emissions

BlueCAM calculates changes to the carbon budget in coastal land following tidal introduction. These changes influence carbon sequestered in soils (Section 1.6) in vegetation (Section 1.5 and influence the emissions of greenhouse gases (GHG's): carbon dioxide (CO_2), methane (CH_4) and nitrous oxide (N_2O) from soils and water bodies (Figure 9). Methane and nitrous oxide have global warming potentials (GWP) 25 and 298 times respectively that of CO_2. In the context of the blue carbon calculator, the production of CH_4 and N_2O is a result of microbial activity. Temperature affects microbial activity and consequently affects the emission rates of all the major GHG's, with higher emissions in warmer/tropical regions and lower emissions in colder/temperate regions, which are reflected in different levels of emissions provided for different climatic regions for coastal wetlands.

Other drivers of GHG exchange for example intensity of eutrophication (nutrient enrichment) or vegetation type and structure, differ for each gas.

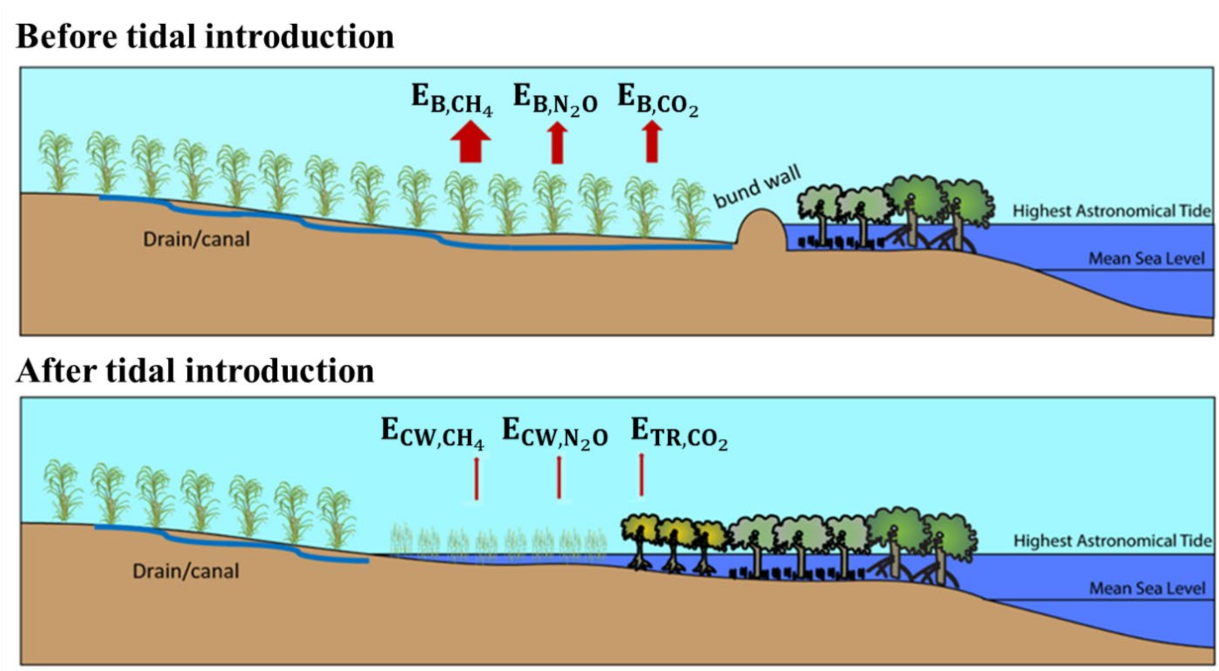

Figure 9: Greenhouse gases considered for baseline and project scenarios in the Blue Carbon Calculator under restoration of coastal wetlands by allowing tidal introduction. Shown here are emissions of methane (E_{B,CH_4}), nitrous oxide (E_{B,N_2O}) and carbon dioxide (E_{B,CO_2}) from baseline land-uses prior to the project, and decreased emissions of methane (E_{CW,CH_4}) and nitrous oxide (E_{CW,N_2O}) from coastal wetlands after tidal introduction, and emissions of carbon dioxide emitted during ecosystem transition (E_{TR,CO_2}). Abatement is calculated as the net difference between emissions before and after restoration (including any project emissions). Diagram adapted from Hagger et al. 2021. Diagram symbols provided by the Integration and Application Network, University of Maryland Center for Environmental Science (available online).

Carbon dioxide - is fixed by plants and carbon is subsequently sequestered in the biomass of plants both above and belowground in roots and ultimately soils. CO_2 is emitted through plant respiration and from the decomposition of organic matter in litter and soils, which is low in anaerobic waterlogged soils and more rapid in aerated soils under freely draining conditions. The removal or mortality of vegetation releases CO_2 as biomass decomposes. The exposure of organic carbon in soils to oxygen through physical disturbance such as drainage and/or tillage significantly increases organic matter decomposition and CO_2 emissions.

Methane - is produced by bacteria in wetlands when organic matter is present and oxygen is not present (anaerobic), which occurs when soils are inundated with water. The production of methane is also limited in the presence of sulphate which occurs in seawater, and thus methane production decreases significantly in waters with high salinity (often above 18ppt). Thus, land areas with high organic matter content (ie. productive vegetated areas) which are inundated with freshwater (eg. freshwater wetlands) are often large source of methane to the atmosphere (eg. CH_4 emissions from flooded agricultural land, managed wet meadow or pasture are high at 325 kg CH_4 ha^{-1} year^{-1}, equivalent to 8.13 MgCO_2e ha^{-1} year^{-1}, compared to CH_4 emissions from grazing land of 3.2 kg CH_4 ha^{-1} year^{-1}, which is equivalent to 0.08 MgCO_2e ha^{-1} year-1, Table 8). The inundation of flooded land areas with tidal waters results in the reduction of methane emissions (as bacteria utilize sulphate in saline water), which are incorporated as avoided emissions in calculating abatement in the blue carbon method.

Nitrous oxide – can be produced under both aerobic and anaerobic conditions through two processes: nitrification (aerobic) and denitrification (anaerobic). Nitrification converts ammonium into nitrate producing nitrous oxide as a by-product and denitrification converts nitrate into nitrogen gas (N_2) with nitrous oxide production as an intermediary product. The major drivers of nitrous oxide (N_2O) production in soils are carbon concentration, nitrogen concentration and soil moisture content. The inundation of land areas with seawater can cease N_2O production from nitrification, however denitrification can still occur if nitrogen is available through ongoing nitrogen inputs. BlueCAM includes N_2O emissions from a range of land-uses prior to tidal introduction as well as from coastal wetlands after tidal introduction consistent with best available scientific evidence.

1.6.1 Estimating abated emissions from coastal wetlands following tidal introduction

Coastal wetlands emit greenhouse gases due to high concentrations of organic matter in soils that is available to support microbial metabolism. Oxidation of sediments during tidal cycles drives CO_2 evasion (fluxes out of the sediment), however this emission is balanced by primary productivity and is therefore not accounted for in equations in BlueCAM (IPCC 2013). Emissions of methane and nitrous oxide partially offset blue C sequestration because both methane and nitrous oxide have a higher global warming potential than CO_2 and are therefore may be specifically accounted for in the calculation of total carbon abatement. Because emissions of methane and nitrous oxide from coastal wetlands are commonly much lower than emissions from freshwater wetlands and agricultural lands abatement of emissions occurs when land is converted to saline coastal wetlands. Although methane and nitrous oxide emissions from coastal wetlands are relatively low compared to many baseline land-uses (Table 9), they are included in the estimation of abatement to achieve accurate estimates of abatement and for completeness.

Abatement in BlueCAM considers GHG emissions occurring from land use in the baseline, during the transition period to coastal wetlands (E_{TR}, section 1.7.3 below), and ongoing emissions from established coastal wetlands (blue carbon ecosystems) for the duration of the crediting period.

1.6.1.1 Baseline land uses

BlueCAM uses emissions factors for baseline land uses which represent the common land types and land uses of the Australian coast (Table 8) and follow similar categorisation of land uses described in IPCC (IPCC, 2013, 2019). Data from published and unpublished sources constraining the exchange of CH_4 and N_2O in Australia from baseline land uses are presented in Table 8. Greenhouse gas emissions from baseline land uses have large variability spatially and temporally due to changes in soil moisture, temperature and other conditions which vary over diel cycles, seasonally and annually. Variability of estimates between studies and the low number of studies result in large variability in estimates of emissions across different land use types and across climate zones. Therefore, median values of emissions were selected from the national data set to represent emissions from each land-use as an accurate approach to estimating abatement as mean values are often influenced by very high values.

Australian data was obtained for all baseline land use categories except for aquaculture ponds that are in production and wild (natural) grasslands. IPCC (2013) guidance indicated as an emission rate from aquaculture ponds of 30 kg CH_4 ha^{-1} yr^{-1} and 0.0017 kg N_2O per kg of fish produced (IPCC, 2019). For land uses with no Australian data available (e.g. emissions from aquaculture ponds that are in production and wild (natural) grasslands), the default value of zero emissions were applied (Table 8). Assuming zero emissions of CH_4 from aquaculture ponds that are in production and wild (natural) grasslands is consistent with theoretical expectations based on high salinity and intense management of ponds that are in production (e.g. use of aerators) and the low nutrient levels in wild (natural) grasslands. The IPCC (2013) links N_2O emissions to aquaculture yields, which are used to estimate GHG emissions from Australian aquaculture systems. Data for methane emissions from aquaculture ponds not in production, from forested lands, grazing land, croplands and drainage ditches and canals are included in Table 8 for accuracy and completeness, but these are not included in the National Greenhouse Gas Inventory, and thus are excluded from estimates of abatement in the blue carbon method.

Table 8 Emission factors based on median values (range in brackets) of methane and nitrous oxide emissions from baseline land uses in Australian coastal land from published and unpublished data.

Baseline land uses	**Emission factor CH_4 (kg ha yr^{-1})**	**n**	**Emission factor N_2O (kg ha yr^{-1})**	**n**
Wetlands				
a) Flooded agricultural land, managed wet meadow or pasture	325.0 (3.3 – 1594.3)	6	14.0 (2.7 – 25.3)	2
b) Ponds and other constructed water bodies*	226.3 (4.4 – 420.5)	2	NA	
d) Aquaculture (in production)	NA		Linked to product yield	
e) Aquaculture (not in production) Saline (if not saline use value for ponds)	-0.1#	1	0.6 (0.2 – 0.6)	3
Forest land				
a) Melaleuca forest	1.2 (-2.2 – 4.7#	2	0.2 (0.2 – 0.3)	2
b) Unmanaged Forest Land	-1.4 (-2.2 - -0.7)#	5	0.7 (0.6 – 1.8)	12
Crop land				
a) Sugarcane	0.0 (0.0 – 44.2)#	3	12.2 (0.0 – 37.8)	11
b) Cropping	0.0 (0.0 – 0.4)#	2	0.7 (0.6 – 1.8)	6
c) Drainage channels or ditches in cropland	62.4#	1	NA	
Grassland				
a) Wild (natural) grasslands	NA		NA	
b) Managed (grazing)	3.2 (-11.3 – 1019.2)#	7	0.3 (0.0 – 1.0)	4

* Includes natural and constructed ponds and tidally restricted fresh and brackish wetlands
# Not included in the National Greenhouse Gas Inventory and thus excluded from estimates of abatement.

1.6.1.2 Coastal wetlands

Australian data on emissions of non-CO_2 GHG emissions from blue carbon coastal wetlands were collected from published and unpublished data sets to calculate emissions factors. Analyses of data indicated that GHG emissions fell into two groups which reflected two climate categories. The two climate categories reflect lower GHG emissions associated with environmental conditions that are generally more saline (arid/semi-arid), cooler (temperate) and less nutrient rich (tropical humid), with higher GHG emissions in region that are warm and less salty (tropical monsoon and subtropical). The median value was used for each climatic category (Table 3). Once tides are introduced, emissions from ditches, drains and canals are assumed to be the same as the wetland community type that establishes with tidal introduction. Because GHG emissions vary with levels of inundation and plant productivity, GHG emissions from mangroves were scaled over the intertidal zone using the same multiplier used for biomass (Table 2). Sparsely vegetated saltmarshes (saltflats) were allocated emission factors of zero given lack of data and theoretical expectations given the high salinity and low soil carbon density in this coastal wetland type. The overall approach gave GHG emission values which were lower than global mean values reported for coastal wetlands across climate zones in IPCC (2013). Lower GHG emissions in Australian coastal wetlands are consistent with the higher salinity (due to aridity) and low nutrient levels in Australian wetlands in comparison with many other global locations where freshwater flows and nutrient enrichment is high. The use of median GHG emissions from two climate regions is accurate as it prevents underestimation of GHG emission from coastal wetlands in the tropical monsoon and subtropics, which would occur if only a single GHG emission value was provided. Greenhouse gas emissions from coastal wetlands are implemented in BlueCAM as a reduction in soil carbon abatement.

Comparison of emissions used in the blue carbon method with those from IPCC Tier 1 values are available in Appendix 3.

Table 9 Emissions based on median values (range in brackets) of methane and nitrous oxide emissions from different climate zones in Australian coastal wetlands from published and unpublished data. Negative values indicate a net sink (uptake) relative to the atmosphere.

NRM climate regions	Emissions CH_4 (kg ha yr^{-1})	n	Emissions N_2O (kg ha yr^{-1})	n
Arid / Semi arid, temperate, tropical humid				
Mangroves	2.19 (0.91 - 3.31)	3	0.24 (0.17 - 2.75)	3
Saltmarsh	0.11 (-0.21 - 0.44)	2	0.13 (0.02 - 0.23)	2
Seagrass	0	1	0	1
Supratidal forest	-2.19	1	0.25	1
Sparsely vegetated saltmarsh (saltflats)	NA		NA	
Tropical monsoon, subtropical				
Mangroves	13.33 (5.01 - 15.51)	3	2.3 (-0.05 - 10.10)	5
Saltmarsh	6.42 (-0.17 - 17.19)	4	2.43 (2.19 - 2.66)	2
Seagrass	0	1	0	1
Supratidal forest	4.64	1	0.18	1
Sparsely vegetated saltmarsh (saltflats)	NA		NA	

1.6.1.3 Emissions from ecosystem transitions

The inundation of vegetated land with seawater causes the mortality of terrestrial vegetation which results in CO_2 emissions from the decomposition of labile components of the biomass. Additionally, transitions from one coastal wetland type to another can occur in the project area as hydrology and bathymetry (water depth) varies with management actions and with sea level rise. When transitions in vegetation type occur, the model assumes that 100% of aboveground biomass of herbaceous vegetation is emitted as CO_2 and that 40% of aboveground biomass of woody vegetation (leaves, branches, fine roots) is emitted as CO_2 following IPCC (2019) and observations that the boles of trees are maintained in the landscape for decades after flooding. The model assumes that carbon stored in the soil is not released as CO_2 when coastal wetland vegetation changes, because soils which are inundated remain anoxic and field evidence suggests higher carbon stocks after coastal wetland transitions (Lamont et al. 2019).

1.6.1.4 Emissions from fuel consumption

Emissions from fuel consumption are calculated separately to the land-based components of BlueCAM using parameters provided by the Clean Energy Regulator. Fuel emissions associated with the project should be subtracted from the net abatement after calculation of the land-based emissions and removals.

References

Adame, M.F., Zakaria, R.M., Fry, B., Chong, V.C., Then, Y.H.A., Brown, C.J. and Lee, S.Y., 2018. Loss and recovery of carbon and nitrogen after mangrove clearing. Ocean & Coastal Management, 161, pp.117-126.

Adame, M.F., Reef, R., Wong, V.N., Balcombe, S.R., Turschwell, M.P., Kavehei, E., Rodríguez, D.C., Kelleway, J.J., Masque, P. and Ronan, M., 2020. Carbon and nitrogen sequestration of Melaleuca floodplain wetlands in tropical Australia. Ecosystems, 23(2), pp.454-466.

Alongi, D.M. (2014) Carbon cycling and storage in mangrove forests. Annual review of marine science 6, 195-219.

Castaneda-Moya et al. 2011. Patterns of Root Dynamics in Mangrove Forests Along Environmental Gradients in the Florida Coastal Everglades, USA. Ecosystems. 14, 1178–1195

Comber, A. et al. (2017) 'Geographically weighted correspondence matrices for local error reporting and change analyses: mapping the spatial distribution of errors and change', Remote sensing letters , 8(3), pp. 234–243.

Comber, A. J., Harris, P. and Tsutsumida, N. (2016) 'Improving land cover classification using input variables derived from a geographically weighted principal components analysis', ISPRS journal of photogrammetry and remote sensing: official publication of the International Society for Photogrammetry and Remote Sensing , 119, pp. 347–360.

Duarte, C.M., Losada, I.J., Hendriks, I.E., Mazarrasa, I., Marbà, N. (2013) The role of coastal plant communities for climate change mitigation and adaptation. Nature Climate Change 3, 961-968.

Fennessy, M.S., Ibánez, C., Calvo-Cubero, J., Sharpe, P., Rovira, A., Callaway, J., Caiola, N. (2019) Environmental controls on carbon sequestration, sediment accretion, and elevation change in the Ebro River Delta: Implications for wetland restoration. Estuarine, Coastal and Shelf Science 222, 32-42.

Hagger V, Waltham N.J., Lovelock C.E. (2021) Opportunities for coastal wetland restoration for blue carbon with co-benefits for 1 biodiversity, coastal fisheries, and water quality. Ecosystem Services, in press

IPCC 2013. 2013 Supplement to the 2006 IPCC Guidelines for National Greenhouse Gas Inventories: Wetlands. Chapter 4: Coastal Wetlands. Intergovenmental Panel on Climate Change, Switzerland.

IPCC 2019. 2019 Refinement to the 2006 IPCC Guidelines for National Greenhouse Gas Inventories. Chapter 7: Wetlands. Intergovernmental Panel on Climate Change, Switzerland.

Kandasamy, K., Rajendran, N., Balakrishnan, B., Thiruganasambandam, R. and Narayanasamy, R., 2021. Carbon sequestration and storage in planted mangrove stands of Avicennia marina. *Regional Studies in Marine Science*, *43*, p.101701.

Kelleway, J.J., Saintilan, N., Macreadie, P.I., Baldock, J.A., Heijnis, H., Zawadzki, A., Gadd, P., Jacobsen, G., Ralph, P.J. (2017) Geochemical analyses reveal the importance of environmental history for blue carbon sequestration. Journal of Geophysical Research: Biogeosciences 122, 1789-1805.

Kennedy, H., Alongi, D.M., Karim, A., Chen, G., Chmura, G.L., Crooks, S., Kairo, J.G., Liao, B., Lin, G., 2014. 2013 Supplement to the 2006 IPCC Guidelines for National Greenhouse Gas Inventories: Wetlands. Chapter 4: Coastal Wetlands. Intergovenmental Panel on Climate Change, Switzerland

Kirwan, M.L., Megonigal, J.P. (2013) Tidal wetland stability in the face of human impacts and sea-level rise. Nature 504, 53-60.

Lamont, K., Saintilan, N., Kelleway, J.J., Mazumder, D. and Zawadzki, A., 2020. Thirty-year repeat measures of mangrove above-and below-ground biomass reveals unexpectedly high carbon sequestration. Ecosystems, 23(2), pp.370-382.

Lal, K.K., Bonetti, C., Woodroffe, C.D. and Rogers, K., 2020. Contemporary distribution of benthic foraminiferal assemblages in coastal wetlands of south-eastern Australia. Estuarine, Coastal and Shelf Science, 245, p.106949.

Lasco, R.D., Ogle, S., Raison, J., Verchot, L., Wassmann, R., Yagi, K., Bhattacharya, S., Brenner, J.S., Daka, J.P., González, S.P., Krug, T., Li, Y., Martino, D.L., McConkey, B.G., Smith, P., Tyler, S.C., Zhakata, W., 2006. 2006 IPCC Guidelines for National Greenhouse Gas Inventories. Volume 4 Agriculture, Forestry and Other Land Use. Chapter 5: Cropland. Intergovernmental Panel on Climate Change, Switzerland.

Mokany, K., Raison, R.J., Prokushkin, A.S., 2006. Critical analysis of root:shoot ratios in terrestrial biomes. Global Change Biology 12, 84-96.

Needelman, B.A., Emmer, I.M., Emmett-Mattox, S., Crooks, S., Megonigal, J.P., Myers, D., Oreska, M.P.J., McGlathery, K. (2018) The Science and Policy of the Verified Carbon Standard Methodology for Tidal Wetland and Seagrass Restoration. Estuaries and Coasts 41, 2159-2171.

Paul, K.I., Roxburgh, S.H., England, J.R., de Ligt, R., Larmour, J.S., Brooksbank, K., Murphy, S., Ritson, P., Hobbs, T., Lewis, T. and Preece, N.D., 2015. Improved models for estimating temporal changes in carbon sequestration in above-ground biomass of mixed-species environmental plantings. Forest Ecology and Management, 338, pp.208-218.

Phan, S.M., Nguyen, H.T.T., Nguyen, T.K. and Lovelock, C., 2019. Modelling above ground biomass accumulation of mangrove plantations in Vietnam. Forest Ecology and Management, 432, pp.376-386.

Preece, N.D., Van Oosterzee, P., Unda, G.C.H. and Lawes, M.J., 2017. National carbon model not sensitive to species, families and site characteristics in a young tropical reforestation project. *Forest Ecology and Management*, *392*, pp.115-124.

Rogers, K., Kelleway, J.J., Saintilan, N., Megonigal, J.P., Adams, J.B., Holmquist, J.R., Lu, M., Schile-Beers, L., Zawadzki, A., Mazumder, D., Woodroffe, C.D. (2019) Wetland carbon storage controlled by millennial-scale variation in relative sea-level rise. Nature 567, 91-95.

Salmo, S.G., Lovelock, C. and Duke, N.C., 2013. Vegetation and soil characteristics as indicators of restoration trajectories in restored mangroves. *Hydrobiologia*, *720*(1), pp.1-18.

Serrano, O., Lovelock, C.E., T, A., Macreadie, P.I., Canto, R., Phinn, S., Arias-Ortiz, A., Bai, L., Baldock, J., Bedulli, C., Carnell, P., Connolly, R.M., Donaldson, P., Esteban, A., Ewers Lewis, C.J., Eyre, B.D., Hayes, M.A., Horwitz, P., Hutley, L.B., Kavazos, C.R.J., Kelleway, J.J., Kendrick, G.A., Kilminster, K., Lafratta, A., Lee, S., Lavery, P.S., Maher, D.T., Marba, N., Masque, P., Mateo, M.A., Mount, R., Ralph, P.J., Roelfsema, C., Rozaimi, M., Ruhon, R., Salinas, C., Samper-Villarreal, J., Sanderman, J., C, S., Santos, I., Sharples, C., Steven, A.D.L., Cannard, T., Trevathan-Tackett, S.M., Duarte, C.M. (2019) Australian vegetated coastal ecosystems as global hotspots for climate change mitigation. Nature Communications 10, 4313.

Sidik, F., Fernanda Adame, M. and Lovelock, C.E., 2019. Carbon sequestration and fluxes of restored mangroves in abandoned aquaculture ponds. Journal of the Indian Ocean Region, 15(2), pp.177-192.

Sillanpää, M., Vantellingen, J. and Friess, D.A., 2017. Vegetation regeneration in a sustainably harvested mangrove forest in West Papua, Indonesia. Forest Ecology and Management, 390, pp.137-146.

Viscarra Rossel, R.A., Webster, R., Bui, E.N., Baldock, J.A. (2014) Baseline map of organic carbon in Australian soil to support national carbon accounting and monitoring under climate change. Global change biology 20, 2953-2970.

Walcker, R., Gandois, L., Proisy, C., Corenblit, D., Mougin, E., Laplanche, C., Ray, R. and Fromard, F., 2018. Control of "blue carbon" storage by mangrove ageing: Evidence from a 66-year chronosequence in French Guiana. *Global change biology*, *24*(6), pp.2325-2338.

Waycott, M., Collier, C., McMahon, K., Ralph, P., McKenzie, L., Udy, J. and Grech, A., 2007. Vulnerability of seagrasses in the Great Barrier Reef to climate change (pp. 193-236). Great Barrier Reef Marine Park Authority and Australian Greenhouse Office.

Woodroffe, C.D., Rogers, K., McKee, K.L., Lovelock, C.E., Mendelssohn, I.A. and Saintilan, N., 2016. Mangrove sedimentation and response to relative sea-level rise. Annual review of marine science, 8, pp.243-266.

Appendix 1 Comparison of carbon stocks, fluxes and GHGs using in the Tidal Introduction BlueCAM and those provided by the IPCC (Tier 1 default values)

Table 10. Comparison of Australian Tidal Introduction BlueCAM approach and IPCC Tier 1 default values for carbon stocks, fluxes, and greenhouse gas fluxes.

	IPCC Approach/Tier 1 value	Australia BlueCAM approach/emission factor
CARBON STOCKS	-	-
***Mangrove Biomass*, tonnes C ha^{-1}**	-	-
Tropical humid	192	167
Tropical monsoon	92	167
Subtropical	75	101
Arid/semiarid	NA	70.3
Temperate	NA	70.4
***Mangrove litter*, tonnes C ha^{-1}**	0.7	NA
***Mangrove dead wood*, tonnes C ha^{-1}**	10.7	NA
Mangrove root:shoot ratio	-	-
Tropical humid	0.49	0.32
Tropical monsoon	0.29	0.32
Subtropical	0.96	0.32
Saltmarsh biomass, tonnes C ha^{-1}	-	-
Tropical, subtropical, arid/semiarid	Use country specific values	1.36
Temperate	Use country specific values	7.89
Saltmarsh root:shoot ratio	-	-
Mediterranean	3.63	Assumed in soil pool
Subtropical	3.65	Assumed in soil pool
Temperate-fresh tidal	1.15	Assumed in soil pool
Temperate	2.11	Assumed in soil pool
***Seagrass biomass, tonnes C* ha^{-1}**	-	-
Tropical, subtropical, semi-arid	Use country specific values	0.2
Temperate, arid	Use country specific values	0.57
Seagrass root:shoot ratio	-	-
Tropical	1.7	Assumed in soil pool
- **Subtropical**	2.4	Assumed in soil pool
- **Temperate**	1.3	Assumed in soil pool
***Supratidal swamp forest biomass*, tonnes C ha^{-1}**	-	-
- **Tropical humid**	NA	192
- **Subtropical**	NA	100

	IPCC Approach/Tier 1 value	Australia BlueCAM approach/emission factor
- **Temperate**	NA	178
Supratidal swamp forest root:shoot ratio	NA	0.32
	-	-
CARBON FLUXES	-	-
***Mangrove biomass growth*, tonnes C ha^{-1} $year^{-1}$**	-	-
- **Tropical humid**	9.9	Use growth curve to mature biomass (above)
- **Tropical monsoon**	3.3	Use growth curve to mature biomass (above)
- **Subtropical**	18.1	Use growth curve to mature biomass (above)
- **Temperate**	NA	Use growth curve to mature biomass (above)
***Supratidal swamp forest biomass growth,* tonnes C ha^{-1} $year^{-1}$**	NA	Use growth curve to mature biomass (above)
***Soil carbon accumulation*, tonnes C ha^{-1} $year^{-1}$**	-	-
- **Mangrove soil carbon accumulation**	1.63	0.95
- **Saltmarsh soil carbon accumulation**	0.91	0.48
- **Seagrass soil carbon accumulation**	0.43	0.21
- **Supratidal forest soil carbon accumulation**	NA	0.61
- **Sparsely vegetated saltmarsh (saltflat) soil carbon accumulation**	NA	0.25
- **Salt evaporation pond soil carbon accumulation**	NA	0
- **Tidally restricted wetland (fresh or brackish) soil carbon accumulation**	NA	0.47
- **Other land-uses soil carbon accumulation**	0	0 (adopt approach of IPCC 2019)
- **Sugarcane land soil carbon losses/emissions**	Soil C stock x 0.61 (over 20 years)	Soil C stock x 0.61 (over 20 years) (adopt IPCC and use Viscarra-Rossel et al. 2014 soil C stocks)
- **Grazing land soil carbon losses/emissions**	Soil C stock x 0.97 (over 20 years)	Soil C stock x 0.97 (over 20 years) (adopt IPCC and use Viscarra-Rossel et al. 2014 soil C stocks)

Table 11 Comparison of Australian Tidal Introduction BlueCAMl approach and IPCC Tier 1 approach for non-CO_2 greenhouse gas emissions

	Methane (kg ha-1 year-1)		**Nitrous Oxide (kg ha-1 year-1)**	
Source	IPCC Approach/Tier 1 emission factor	Australia BC abatement model approach/emission factor	IPCC Approach/Tier 1 emission factor	Australia BC abatement model approach/emission factor
Mangrove	-	-	-	-
tropical humid, arid/ semiarid, temperate	193.7	2.19	NA	0.24
tropical monsoon, subtropical	193.7	13.3	NA	2.3
Saltmarsh	-	-	-	-
tropical humid, arid/ semiarid, temperate	193.7 (Wetlands 136-153)	0.11	NA	0.13
tropical monsoon, subtropical	193.7	6.42	NA	2.43
Seagrass	NA	0	NA	0
Supratidal swamp forest	-	-	-	-
tropical humid, arid/ semiarid, temperate	41.2	-2.19	NA	0.25
tropical monsoon, subtropical	41.2	4.64	NA	0.18
Unmanaged forest	0	-1.4	0	0.7
Melaleuca forest	41.2	1.2	0	0.2
Ditches, drains, channels	416	62.4	NA	NA
Saline ponds	30	-0.1	NA	0.6
Freshwater and brackish ponds	183	226	NA	NA
Flooded agricultural land, managed wet meadow or pasture	-	-	-	-

	Methane (kg ha-1 year-1)		**Nitrous Oxide (kg ha-1 year-1)**	
Source	IPCC Approach/Tier 1 emission factor	Australia BC abatement model approach/emission factor	IPCC Approach/Tier 1 emission factor	Australia BC abatement model approach/emission factor
tropical	900	325	NA	14
temperate	235	325	NA	14
Managed grassland (drained/grazing)	2.5 - 4.9	3.2	1.6 - 9	0.3
Natural grassland	1.8 – 39* (*nutrient rich)	NA (use managed grassland)	1.6 - 9	NA (use managed grassland)
Sugarcane	7	0	2.4 - 13	12.2
Other crops	7	0	2.4 - 13	0.7

Appendix 2 Case Studies

Appendix 2.1 Salt field, tidal reconnection trial

S Dittmann & L. Mosley

Introduction

The tidal reconnection of a former salt pond XB8A commenced in July 2017, following the cessation of salt production in 2013. The pond is part of the Dry Creek salt field which extends over 25 km along the coast north of Adelaide and encompasses an area of 4,224 ha of ponds (3,598 ha excluding the crystalliser ponds) (Figure 10a). Operation of the solar evaporation ponds commenced in 1937, with water intake occurring initially at pond XB8A, before being relocated north as the salt field expanded (Mosley et al. 2019, 2020). Seaward ponds in the middle section of the salt field were considered more suitable for restoration to tidal wetlands than those near the former crystalliser ponds, where salt harvesting took place. Ceasing of salt production also offered the opportunity to achieve carbon sequestration through tidal reconnecting of large sections of the salt field (Dittmann et al. 2019a, 2020).

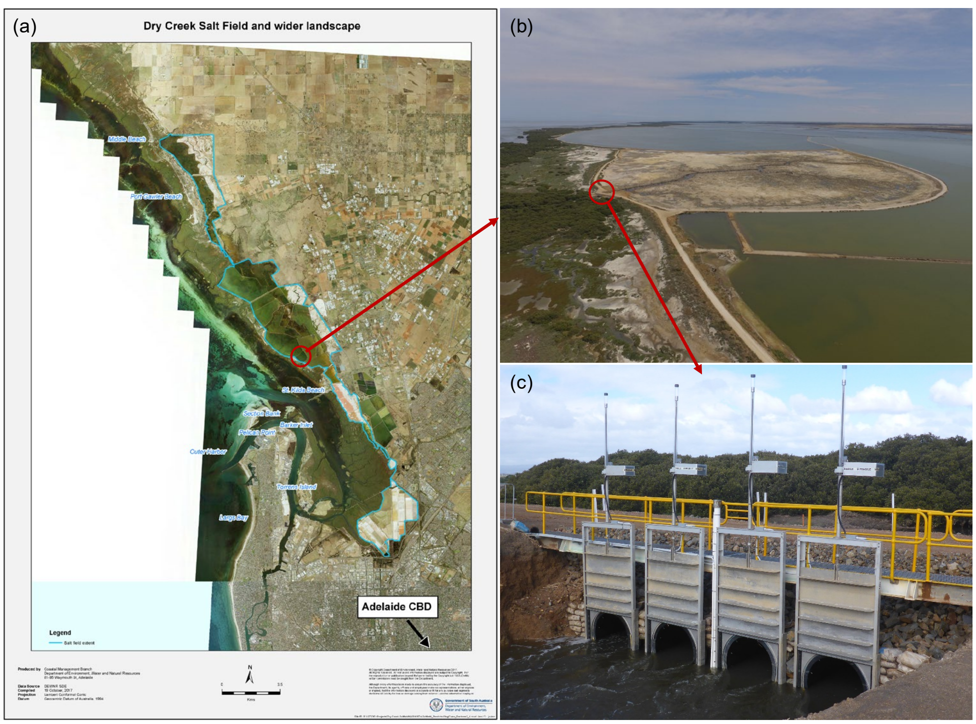

Figure 10: (a) Location of the Dry Creek salt field, South Australia, encircled by blue line. Red circle indicates trial pond XB8A. (b) Trial pond XB8A a few months after tidal reconnection. (c) controllable tidal gates allowing regular cycling of tides in and out of the trial pond.

Pond XB8A was reconnected to the Gulf of St Vincent with a tidal gate infrastructure that allowed control of water entering and exiting the pond, as required by regulatory authorities (Figure 10 b, c). Introducing tidal cycling was also a trial to remediate hypersaline and monosulfidic conditions which had developed during decades of salt field operation (Mosley et al. 2015). The infrastructure consists of 4 x 1.2 m diameter x 10 m long polyethylene pipes and controllable tidal gates (AWMA i-gate), powered by solar panels. Engineering design calculations provided the pipe sizing, orientation, and elevation for suitable water exchange within the typical tidal ranges (Mosley et al. 2020). A multi-parameter water quality sensor (YSI EXO2) was installed on the pond side of the gate, with level sensors also installed on both sides of the gate. No adverse effects on water quality were recorded since reintroduction of tidal flow (Mosley et al. 2020).

Carbon Abatement

Effects on carbon stocks were followed to assess Blue Carbon potential from tidal reconnection of the salt pond. The trial pond XB8A has an area of ~31 ha, which was not divided into carbon abatement areas (CEA)[1]. Two carbon pools were considered, soil and live above-ground biomass. Because of the hypersaline conditions, methane fluxes were not included in carbon abatement assessments.
Soil organic carbon was first measured in soils inside the trial pond three months before reconnection as a baseline, and on six occasions over the 2.7 years since reconnection. Soil organic carbon was also sampled from an adjacent pond operating as business as usual. Following tidal reconnection, soil carbon stocks increased, although the rate of increase varied within the pond (Figure 11a). Calculated to the 30 ha pond area, and two periods about 1 year apart, the net soil carbon sequestration after nearly three years of tidal reconnection was 4086 t CO_2 equivalent (CO_2e, Figure 11b), or approximately 45 t CO_2e ha^{-1} year^{-1}.

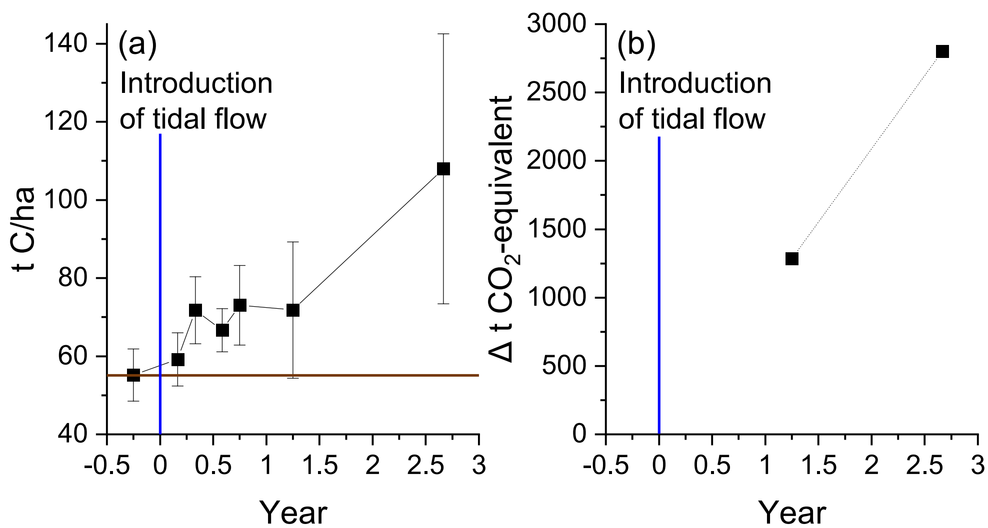

Figure 11: (a) Soil carbon stock (mean ± standard error, n=6) in the trial pond XB8A of the Dry Creek salt field over the first 3 years after tidal reconnection. Based on soil cores to 30 cm depths. (b) Carbon stock change in CO_2 equivalent for the pond area (30 ha) determined for two consecutive time periods of 1.08 and 1.42 years.

For the biomass carbon pool, the baseline was zero, as no vascular plants occurred in the pond prior to tidal reconnection (Figure 12a). Remnants of mangrove trees along the central creek were considered necromass as they died in the 1930s when the pond was flooded to become a salt evaporation pond. No planting occurred, and revegetation commenced naturally through seed dispersal. Mangrove propagules

[1] The trial pond was initially divided into three strata (CEA) based on elevation levels and predicted vegetation cover from nearby areas (Dittmann et al. 2019a). These corresponded to Mangrove-low marsh (20 ha), Tidal saltmarsh (6 ha), and Supratidal saltmarsh (4 ha). More accurate bathymetry from airborne LiDAR three years after tidal reconnection indicated a larger area of the Tidal saltmarsh stratum (16 ha), and a smaller Mangrove-low marsh stratum (11 ha). As it remains unknown whether these measurements document a real change in elevation, a conservative approach was taken, and strata not differentiated within the 31 ha pond (Dittmann et al. 2020).

have been washed into the trial pond by the tides, but not yet established. Saltmarsh is dominated by early colonising species (*Salicornia quinqueflora*, *Suaeda australis*). Nearly three years after introducing tidal flow, 6.23 ha of the 31 ha pond were covered by saltmarsh (Figure 12b). The net carbon stock change from saltmarsh equated to 13.16 t C/yr. While the net abatement from saltmarsh biomass of 48.24 t CO_2e since tidal reconnection is immaterial compared to the soil carbon abatement over the same time, further revegetation is occurring, including of more woody shrubs (*Tecticornia arbuscula*) (Figure 12c, d) (Dittmann et al. 2020).

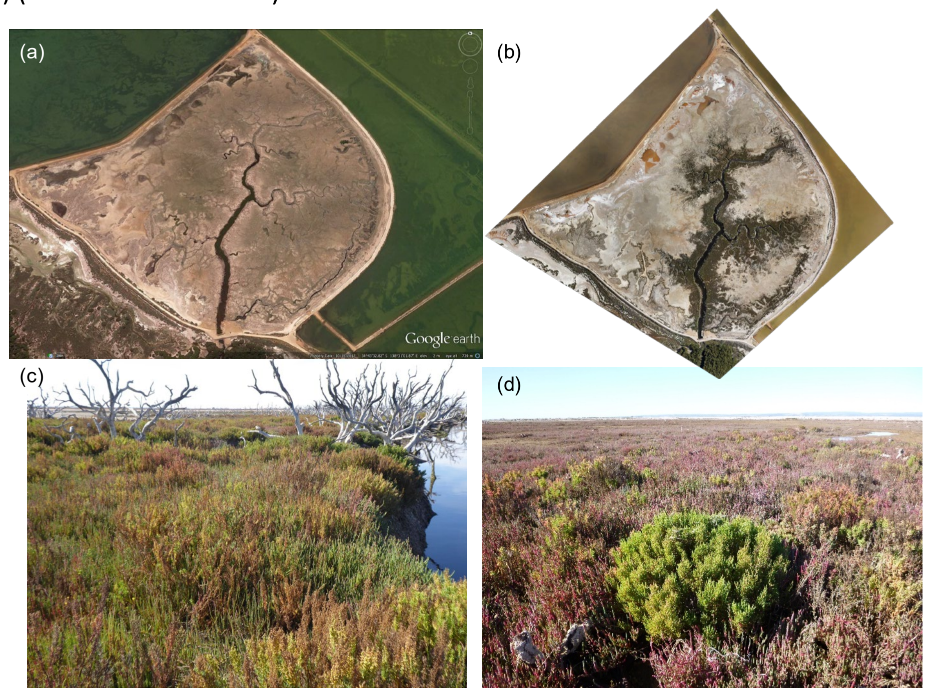

Figure 12: (a) Google Earth image of the trial pond shortly after tidal gates were installed, with no vegetation present. (b) RGB image from Airborne Research Australia, showing revegetation along the creeks in the trial pond, nearly three years after introduction of tidal flow. (c) dense saltmarsh vegetation adjacent to the central creek. (d) Young plants of Tecticornia arbuscula (photo Kieren Beaumont).

As tidal reconnection of the trial pond XB8A occurred before a blue carbon project under the ERF was possible, it serves as an important pilot project documenting carbon stock changes after tidal reconnection, which will support improved modelling and default values in the future. The possible carbon abatement for larger sections of the salt field was modelled based on data from the pond and a mangrove chronosequence (see case study for Swan Alley) and considering sea level rise at RCP 8.5. The models showed that the hypothetical tidal reconnection of larger areas (~2000 ha) of the salt field could gain carbon abatement of >500,000 t CO_2-equivalent over the crediting time, and that permanence can be best assured by providing landward retreat (Dittmann et al. 2019b).

References

Dittmann, S., L. Mosley, K. Beaumont, B. Clarke, E. Bestland, et al. 2019a. From Salt to C; carbon sequestration through ecological restoration at the Dry Creek Salt Field. Goyder Institute for Water Research Technical Report Series No. 19/28.

Dittmann, S., L. Mosley, M. Clanahan, J. Quinn, S. Crooks, et al. 2019b. Proof of concept for tidal re-connection as a blue carbon offset project. Goyder Institute for Water Research Technical Report Series No. 19/29.

Dittmann, S., Beaumont, K., Mosley, L., Leyden, E., Jones, A., et al. 2020. A Blue Carbon future through introducing tidal flow to salt ponds and stranded samphire for Dry Creek and the Samphire Coast. Report for the Adelaide and Mt Lofty Ranges NRM Board and Green Adelaide.

Mosley, L.M., P. Marschner, & R.W. Fitzpatrick. 2015. Research to inform a tidal cycling trial at the Dry Creek salt ponds. Report to the Department for Environment Water and Natural Resources. University of Adelaide Acid Sulfate Soil Centre.

Mosley, L., B. Thomas, R. Fitzpatrick, & Quinn J. 2019. Pathways to tidal restoration of the Dry Creek salt field. Report to the Department for Environment and Water.

Mosley, L., T. Dang, P. Marschner, R. Fitzpatrick, & Quinn J. 2020. Environmental outcomes from a tidal restoration trial at the Dry Creek salt field. Report to the Department for Environment and Water and Adelaide-Mt Lofty Ranges Natural Resources Management Board. The University of Adelaide.

Appendix 2.2 Case Study in South Australia – Chronosequence after tidal reconnection

S Dittmann, K. Beaumont & L. Mosley

Introduction

The Swan Alley area in the Barker Inlet, South Australia, was isolated from tidal flows by a levee bank built in 1895 with the intent of reclaiming swamp land for agriculture (Burton 1982). At the time of construction, the levee followed the landward extent of mangrove vegetation. The levee was first breached by storms between 1914 and 1918 and abandoned in 1935 (Fitzpatrick et al. 2008), which allowed natural colonisation with mangroves in the Swan Alley area. Introduction of tides combined with land subsidence and sea-level rise enabled the mangrove encroachment (Burton 1982, Belperio 1993). Analyses of a historical aerial photos allowed to reconstruct the decadal increase in mangrove cover following tidal reconnection in the 1930s (Clanahan 2019) (Figure 13).

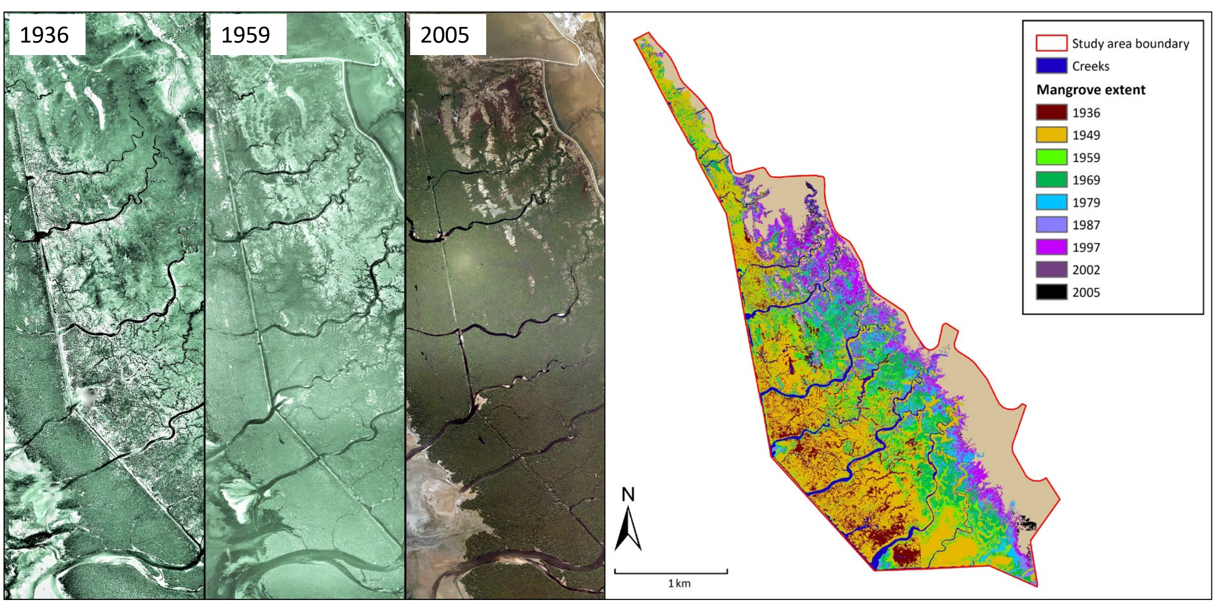

Figure 13: Mangrove colonisation following tidal introduction through breached levee banks in the Swan Alley area in Barker Inlet, South Australia. Examples of orthorectified aerial photographs for three time periods, and a composite map for mangrove extent of several decades, based on Clanahan 2019.

Carbon Abatement

The chronosequence at Swan Alley offers a unique 'space-for-time substitution' opportunity to determine mangrove growth rates and carbon stock increase in mangrove biomass and soils. For each forest age decade, three replicate sites were sampled. Measurements were also taken outside of the former levee bank in mature mangrove estimated to be >100 years old.
The mature mangrove forest had an average above ground carbon stock of 117.6 ± 16.18 t C/ha (Dittmann et al. 2020). In the recolonised mangrove forest following tidal reintroduction, the above-ground carbon stock increased linearly with forest age with a predicted carbon accumulation rate (from slope parameter of linear regression) of 1.18 t C/ha/yr, and reached about 100 t C/ha after several decades (Figure 14a). The average soil organic carbon stock of the mature forest was 157.03 t C/ha. Soil organic carbon in the colonising mangrove forest after tidal reconnection increased annually by 1.43 t C/ha/yr based on a linear regression (Figure 14b).

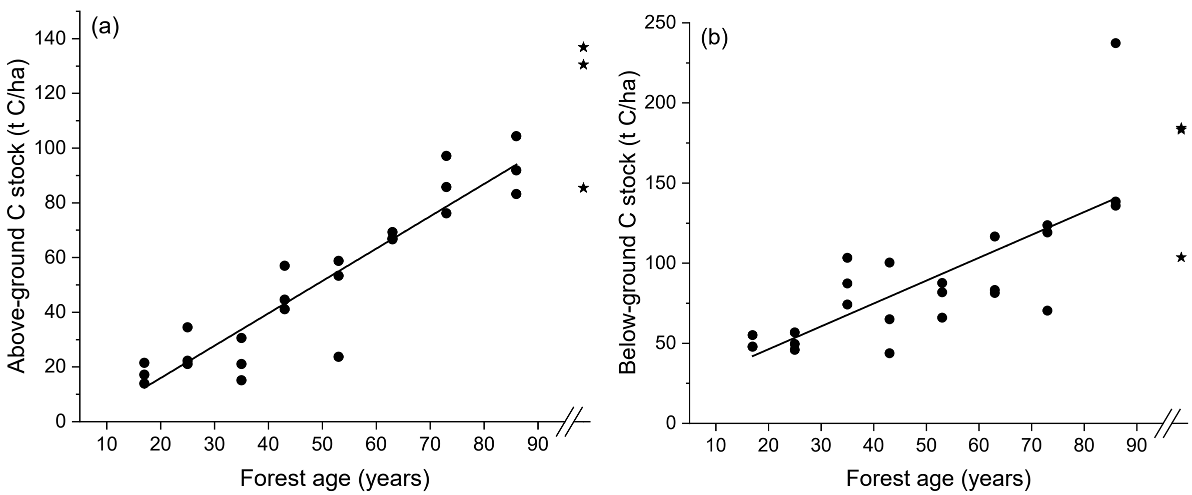

Figure 14: Carbon stock (t C/ha) in a) above-ground biomass and b) soil (to 50 cm), along a chronosequence of Avicennia marina at Swan Alley. The x-axis break separates the mature mangrove (✶) forest seaward from the levy bank, which has an unknown age but is estimated to be >100 years. From Dittmann et al. 2020.

The assessment of above- and belowground carbon stocks for the different forest ages at the Swan Alley chronosequence indicates that introducing tidal flow has long-term benefits for carbon sequestration. The accumulation rates for biomass and soil carbon from the chronosequence informs modelling of long-term carbon stock changes and permanence of the Blue Carbon method.

References

Belperio, A.P. 1993. Land subsidence and sea level rise in the Port Adelaide estuary implications for monitoring the greenhouse effect. *Australian Journal of Earth Sciences* 40: 359-368

Burton, T.E. 1982. Mangrove development north of Adelaide, 1935-1982. *Transactions of the Royal Society of South Australia* 106: 183-189

Clanahan, M. 2019. Combining remote sensing and field surveys to describe decadal mangrove changes following reconnection of a wetland. Honours Thesis, Flinders University Adelaide

Dittmann, S., Beaumont, K., Mosley, L., Leyden, E., Jones, A., et al. 2020. A Blue Carbon future through introducing tidal flow to salt ponds and stranded samphire for Dry Creek and the Samphire Coast. Report for the Adelaide and Mt Lofty Ranges NRM Board and Green Adelaide.

Fitzpatrick, R.W., B.G. Thomas, R.H. Merry, and S. Marvanek. 2008. Acid sulfate soils in Barker Inlet and Gulf St. Vincent priority region. Report prepared for Commonwealth Scientific and Industrial Research Organisation (CSIRO). CSIRO Land and Water Science Report Series, report no. 35/08. CSIRO, Adelaide, South Australia.

Appendix 3 Further information on soil carbon

Case study: CAR in wetlands with restrictions to tidal flows

Preliminary radiometric dating data from tidal restoration locations in the Hunter River estuary, NSW (temperate zone) show soil accumulation can occur during baseline (tidal restriction) conditions (Table 10). For zones that have restored to saltmarsh at both Kooragang Island (tidal restoration from 1995) and Hexham (tidal restoration from 2009), mass accumulation was similar or higher during the decades of tidal restriction compared to post-restoration estimates. The potential for carbon additions below dated horizons precludes definitive estimates of carbon accumulation rates for each phase, however, application of a carbon factor integrated over the entire age-depth model range (i.e. encompassing pre-restriction, restriction and restored soil depths), shows similar trends to MAR estimates. Notably, each of the CAR estimates is greater than the national mean saltmarsh CAR reported by Serrano et al. (2019).

Similarly, there is evidence of mass accumulation during the tidal restriction phase for the zone at Hexham which has subsequently restored to a young mangrove forest. Post-restoration accumulation rates have increased markedly here, relative to the tidal restriction phase.

Table 12 Comparison of Mass (MAR) and Carbon (CAR) accumulation rates for three tidal restoration settings in the Hunter estuary, NSW. MAR is derived from radiometric dating, while CAR estimates are calculated as MAR x mean carbon concentration (%C) of the depth range of the radiometric dating for each core. (Source: J. Kelleway, unpublished data.)

	MAR		**CAR estimate**	
	(g cm^{-2} y^{-1})	±	(Mg C ha^{-1} y^{-1})	±
Kooragang (restored saltmarsh)				
entire ^{210}Pb record	0.107	0.008	0.80	0.06
post-restoration	0.102	0.007	0.76	0.05
restriction	**0.118**	0.011	**0.88**	0.08
Hexham (restored saltmarsh)				
entire ^{210}Pb record	0.109	0.027	0.64	0.16
post-restoration	0.086	0.007	0.51	0.04
restriction	**0.096**	0.012	**0.57**	0.07
Hexham (restored mangrove)				
entire ^{210}Pb record	0.059	0.002	0.63	0.02
post-restoration	**0.100**	0.006	**1.07**	0.06
restriction	0.055	0.006	0.59	0.06

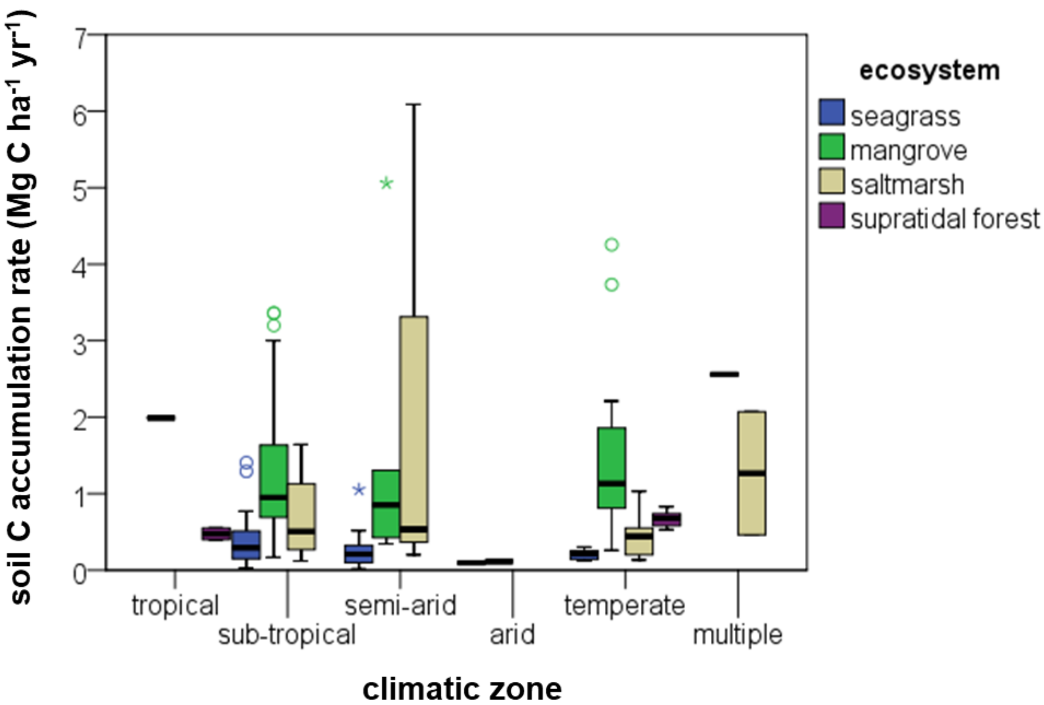

Figure 15: Box and whisker plot of Australian soil carbon accumulation rates by ecosystem type and climatic zone. Solid horizontal lines within each box represent the median estimate. Stars and circles represent extreme values and potential outliers respectively. The 'multiple' climatic zone incorporates pooled estimates incorporating a small number of temperate and sub-tropical sites (Saintilan et al. 2013).

Is it appropriate to use data from natural systems (rather than restored systems) to develop modelled soil carbon accumulation parameters?

Mangrove

Review of the literature and data from Serrano et al. (2019) provided a range of data to assess whether restored sites have soil carbon accumulation rates that are different to those of natural sites. Assessment of nine studies from eight countries where soil carbon accumulation in natural sites was compared to restored or newly established mangrove habitat found no significant difference (Table 13). Studies from Australia in this data set are from South Australia (Mutton Creek) and New South Wales (Kooragang, Hexham).

Using a larger data set, including those that permitted a comparison of pairs (above) as well as data from Serrano et al. (2019) and those where natural sites were not assessed in the same study, resulted in a similar conclusion. Natural sites accumulate soil carbon at a slightly higher but statistically similar rate as those mangroves that are restored or early in their development (Table 12). Australian sites were well represented in both data sets.

Table 13 Comparison of soil carbon accumulation rates in restored and natural mangrove sites.

	Soil C accumulation Mg C ha^{-1} year^{-1}			
Data set	**Restored**	**Reference/older**	**Test**	**Notes**
Global Data where paired data were available	1.94 ± 0.89	1.73 ± 0.48	Paired t test t= 0.269, P= 0.794, df=9	8 countries, 3 of 10 observations from Australia
Global Data (not paired)	2.44 ± 0.77 (N=17)	1.94 ± 0.39 (N = 47)	ANOVA $F_{1,58}$ = 0.025; P=0.875	12 countries, 35 of 70 observations from Australia
Serrano et al. 2019, overall mean	-	1.26 ± 0.18 (N=24)	-	All climatic zones

Saltmarsh

Global analysis has demonstrated that Australian saltmarshes store and accumulate soil carbon in different volumes and rates to more data-rich regions of the northern hemisphere (i.e. North America and Europe)(Rogers et al., 2019). This precludes a meaningful comparison of global data for restored versus natural tidal marshes in the context of Australian settings. Limited data is currently available for Australia, precluding statistical analysis, and is presented in Table 13. Broadly, this data suggests national mean estimates of undisturbed saltmarshes are more likely to represent an underestimate (rather than overestimate) of soil carbon accumulation rates in restored settings.

Table 13 Comparison of soil carbon accumulation rates in Australian restored and natural saltmarsh sites.

	Soil C accumulation Mg C ha^{-1} year^{-1}			
Data set	**Restored**	**Reference**	**Method**	**Notes**
Gulliver et al. 2020, Snake Island, VIC	1.02 ± 0.75	0.54 ± 0.22	Radiometric dating	Restored = 9 years post tidal restoration; Reference = 65 years post tidal restoration
Howes et al. 2009, Kooragang Island, NSW	1.37	0.64	Marker Horizon	~11 years post restoration
J. Kelleway et al. unpublished, Kooragang Island, NSW	0.76 ± 0.05	1.64 ± 0.23	Radiometric dating	22 years post restoration
J. Kelleway et al. unpublished, Hexham, NSW	0.51 ± 0.04	n.d.	Radiometric dating	8 years post restoration
Serrano et al. 2019, overall mean	-	0.39 ± 0.3	various	All climatic zones. Based upon modelled data